
ACCELERATED PATHS AND UNRUH EFFECT: FINITE TIME DETECTOR RESPONSE IN (ANTI) DE SITTER SPACETIME AND HUYGEN'S PRINCIPLE.

A PREPRINT

Shahnewaz Ahmed,^{a,b,c} Mir Mehedi Faruk,^{d,e,f} and Muktadir Rahman^g

^aSchool of Data and Sciences, BRAC University, 66 Mohakhali, Dhaka 1212. Bangladesh

^bPerimeter Institute for Theoretical Physics, Waterloo, ON N2L 2Y5, Canada

^cDepartment of Physics and Astronomy, University of Waterloo, Waterloo, Ontario N2L 3G1, Canada

^dDepartment of Physics, McGill University, Montreal, Quebec, H3A 2T8, Canada

^eInstitute for Theoretical Physics, University of Amsterdam, Science Park 904, 1090 GL Amsterdam, The Netherlands.

^fDelta Institute for Theoretical Physics, Science Park 904, PO Box 94485, 1090 GL Amsterdam, The Netherlands.

^gDepartment of Physics, University of Nevada, Reno 1664 N Virginia St, Reno, NV 89557.

April 28, 2023

ABSTRACT

We study the finite time response of an Unruh-DeWitt particle detector described by a qubit (two-level system) moving with uniform constant acceleration in maximally symmetric spacetimes. The D dimensional massless fermionic response function in de Sitter (dS) background is found to be identical to that of a detector linearly coupled to a massless scalar field in $2D$ dimensional dS background. Furthermore, we visit the status of Huygen's principle in the Unruh radiation observed by the detector.

A uniformly accelerating observer of constant acceleration a moving in Minkowski or maximally symmetric spacetime sees the vacuum for an inertial observer as a thermal state of temperature $T = \frac{\omega}{2\pi}$. Here, ω is given by [1, 2, 3, 4, 5, 6],

$$\omega = \begin{cases} \sqrt{a^2 + k^2}, & \text{dS, } \Lambda > 0 \\ \sqrt{a^2 - k^2} & \text{AdS, } \Lambda < 0 \\ a & \text{Minkowski, } \Lambda = 0 \end{cases} \quad (1)$$

Here the cosmological constant Λ is related to D dimension spacetime curvature, k through $|\Lambda| = \frac{k^2}{2}(D-2)(D-3)$. In recent times, Unruh radiation and its close analogue Hawking radiation has been extensively studied with the tool of the Unruh-Dewitt (UDW) particle detector. The UDW detector has applications connecting other branches of physics including but not limited to understanding harvesting entanglement [7, 8, 9, 10], QCD [11], complexity [12], cosmology [13, 14, 15], as well as in application-oriented research directions such as condensed matter systems [16, 17] like anyons [18] and constructing heat engines [19, 20] using UDW detector. The accelerated UDW detector shows a response when coupled to matter field. In one of the pioneering work on the topics related to detector physics was by Takagi [21] where interesting features of detector response function were elaborated. A complete story on fermionic response function to accelerated detectors in flat spacetime was developed recently in [22]. It was noted in that [22] in D -dimensional Minkowski spacetime, the

response of the accelerated UDW detector coupled to massless Dirac field proportional to that of a detector linearly coupled to a massless scalar field in $2D$ dimension. This observation was quite interesting as it helped us measure the Unruh radiation observed by the detector when coupled to the fermionic matter field. But it is a natural question to ask if a similar conclusion also arises when the fermionic field is coupled to curved spacetime. In our previous article[23] we explained how the same mechanism works in AdS background instead. Another significant observation made by several authors[24, 25] is the apparent statistics inversion in the Unruh radiation in odd dimensional spacetime. In odd-dimensional spacetime, we notice that the thermal radiation measured by a linear UDW particle detector coming from scalar field can maintain an anti periodic relation. Our previous article explained how non-linearity affects the statistics inversion in AdS spacetime. Of course, when the curvature of the spacetime was approaching zero, we reproduced the known results of detector response in flat spacetime[6, 23] but the similar setup in the dS background still needs to be discussed. In this article, we analyze the effects of non-linearity and develop the calculation of the fermionic response function in the dS background. In our earlier work and many other studies relating to the UDW detector, we investigated the response function where the detector is "turned on" for an infinite amount of time [6, 21, 23]. In practice it is impossible to turn on the detector for infinite time[20]; therefore, the finite time response has been rigorously investigated in the context of flat space time [26]. We start our manuscript by analysing the finite time response of accelerated an UDW detector in AdS spacetime coupled to real scalar fields in a non-linear way. In section 2, we first elaborate on the dS case for the real scalar fields and then finish the calculation for fermionic fields. We prove here the response function of the uniformly accelerated UDW detector coupled to a massless Dirac field in dS spacetime of dimension is equivalent to the response function of the detector linearly coupled to a massless scalar field in $2D$ dimensional dS spacetime. We have generalised the result in the case of non trivial gravitational background AdS spacetime in part-1[23] and dS spacetime in this article. Finally, we summarise the cases when the Huygens principle is maintained or violated by the Unruh radiation observed by the accelerated detectors in maximally symmetric spacetime. We point out that fermionic Unruh radiation respects the Huygens principle in any dimension, unlike scalar theory. We explain here the reason behind.¹ Throughout the whole article, we chose $\hbar = 1$, $c = 1$ and Boltzmann constant $k_B = 1$ in our calculation.

1 Finite time response of UDW detector: Scalar field

We first consider a real scalar field Φ in D dimensional (A)dS spacetime which is conformally coupled to gravitational background. We are considering the AdS metric in Poincare coordinates but we can ofcourse choose any other coordinates system such as global coordinates. Similarly we will follow the flat slicing for De Sitter background. The AdS metric in Poincare coordinate,

$$ds^2 = \frac{1}{k^2 z^2} (dt^2 - dx_1^2 - dx_2^2 - \dots - dx_{D-2}^2 - dz^2). \quad (2)$$

The dS metric in flat slicing is written as

$$ds^2 = \frac{1}{k^2 \eta^2} (d\eta^2 - dx_1^2 - dx_2^2 - \dots - dx_{D-2}^2 - dx_{D-1}^2). \quad (3)$$

Depending upon what we would like to have as our our gravitational background we pick AdS or dS we choose eq.(2) or eq. (3). The total action of our system of interest is,

¹In previous study, (see ref.[25]), it was claimed that the Huygens principle is violated (satisfied) in even (odd) dimensions for fermionic Unruh radiation. We show here that it is not the case.

$$S = S_0 + S_{int} + S_{detector}, \quad (4)$$

The matter field action is simply-

$$S_0 = \frac{1}{2} \int d^D x \sqrt{|g|} (g^{\mu\nu} \nabla_\mu \Phi \nabla_\nu \Phi + \zeta R \Phi^2). \quad (5)$$

When scalars are conformally coupled to gravity one can specify[27],

$$\zeta = \frac{D-2}{4(D-1)}. \quad (6)$$

The interaction part of the Hamiltonian is simply,

$$H_I(\tau) = \lambda \chi_{\mathcal{T}}(\hat{\sigma}^-(\tau) + \hat{\sigma}^+(\tau)) \Phi(z(\tau)), \quad (7)$$

where, λ is the strength of coupling, $\chi_{\mathcal{T}}$ is a switching function which controls the time of interaction with the field, and n is any positive integer. \mathcal{T} represents how long the detector is on. We are going to refer it as switching time. It is well known that any sudden jump in the switching function may cause divergence[20] for finite time interaction. Therefore we choose a Lorentzian switching function (a smooth function),

$$\chi_{\mathcal{T}}(\tau) = \frac{(\mathcal{T}/2)^2}{\tau^2 + (\mathcal{T}/2)^2} \quad (8)$$

One can simply set $\mathcal{T} \rightarrow \infty$, or $\chi_{\mathcal{T}} = 1$ in order to obtain the usual detector response (where it is assumed that the detector can interact with the matter fields for infinite time). The detector is thought as a two-level quantum system defined along a worldline $x(\tau)$. The detector Hamiltonian is,

$$\hat{H}_D = \frac{\Omega}{2} (\hat{\sigma}^+ \hat{\sigma}^- - \hat{\sigma}^- \hat{\sigma}^+), \quad (9)$$

We are thinking the UDW detector as two level system. There are two states $|g\rangle$ and $|e\rangle$ and Ω is the energy gap between these two states. The $\hat{\sigma}^+$ and $\hat{\sigma}^-$ are the well known $SU(2)$ ladder operators.

$$|e\rangle = \hat{\sigma}^+ |g\rangle, \quad (10)$$

$$\hat{\sigma}^- |g\rangle = 0 \quad (11)$$

From this Hamiltonian we can easily see the ground and excited states of the detector are $|g\rangle$ and $|e\rangle$, respectively.

$$\hat{H}_D |e\rangle = \frac{\Omega}{2} |e\rangle \quad (12)$$

$$\hat{H}_D |g\rangle = -\frac{\Omega}{2} |g\rangle \quad (13)$$

Point to note that \hat{H}_D generates time translations with respect to the detector's proper time τ . We are assuming that the detector follows a timelike trajectory $x(\tau)$ which parametrized by proper time τ in D dimensional spacetime. Any real scalar quantum field $\Phi(x)$ can be written as a mode expansion,

$$\Phi(x) = \int d^l k \left(f_k(x) \hat{b}_k + f_k^*(x) \hat{b}_k^\dagger \right), \quad (14)$$

where $\{u_k(x)\}$ is assumed to be a normalized basis of solutions to the Klein-Gordon equation. The functional form is fixed from the gravitational background. the annihilation and creation

operators maintaining the usual commutation relations are $\hat{b}_k, \hat{b}_k^\dagger$, respectively. In principle the creation/annihilation operators help can be used construct a Hilbert space representation for the quantum field, defined in terms of the vacuum state $|0\rangle$. The most interesting quantity to us is the probability amplitude related to the transition from the initial state $|g, 0\rangle$ to a state $|e, \varphi\rangle$. Here $|\varphi\rangle$ denotes an arbitrary final state of the field. The amplitude can be found following[28],

$$\begin{aligned} \mathcal{A}_{g \rightarrow e}(\varphi) &= \langle e, \varphi | U_I | g, 0 \rangle = \sum_{n=0}^{\infty} \langle e, \varphi | U_I^{(n)} | g, 0 \rangle \\ &= \sum_{n \text{ odd}} \lambda^n \frac{(-i)^n}{n!} \int d\tau_1 \cdots d\tau_n \chi(\tau_1) \cdots \chi(\tau_n) \langle \varphi | \mathcal{T} \left(\hat{\phi}(\tau_1) \cdots \hat{\phi}(\tau_n) \right) | 0 \rangle e^{i\Omega(\tau_1 - \tau_2 + \cdots + \tau_n)}, \end{aligned} \quad (15)$$

Here U_I the time evolution operator is given in the usual way,

$$U_I = \mathcal{T} \exp \left(-i \int d\tau H_I(\tau) \right) = \sum_{n=0}^{\infty} \frac{(-i)^n}{n!} \int d\tau_1 \cdots d\tau_n \underbrace{\mathcal{T} \left(H_I(\tau_1) \cdots H_I(\tau_n) \right)}_{U_I^{(n)}} = \sum_{n=0}^{\infty} U_I^{(n)} \quad (16)$$

One can determine the transition probability to arbitrary order by tracing over the field final states $|\varphi\rangle$,

$$\begin{aligned} \mathcal{P}_{g \rightarrow e} &= \int \mathbf{D}\varphi |\mathcal{A}_{g \rightarrow e}(\varphi)|^2 \\ &= \sum_{n, m \text{ odd}} \lambda^{n+m} \frac{(-i)^{n-m}}{n!m!} \int d\tau'_1 \cdots d\tau'_m d\tau_1 \cdots d\tau_n \chi(\tau'_1) \cdots \chi(\tau'_m) \chi(\tau_1) \cdots \chi(\tau_n) \\ &\quad \times \langle 0 | \mathcal{T} \left(\Phi(\tau'_1) \cdots \Phi(\tau'_m) \right)^\dagger \mathcal{T} \left(\Phi(\tau_1) \cdots \Phi(\tau_n) \right) | 0 \rangle e^{-i\Omega(\tau'_1 - \cdots + \tau'_m)} e^{i\Omega(\tau_1 - \cdots + \tau_n)}, \end{aligned} \quad (17)$$

In this series the lowest order term is of second order in the coupling constant λ . It is expressed as,

$$\mathcal{P}_{g \rightarrow e}^{(2)} = \lambda^2 \int d\tau d\tau' \chi(\tau) \chi(\tau') \langle 0 | \Phi(\tau) \Phi(\tau') | 0 \rangle e^{i\Omega(\tau - \tau')} = \lambda^2 \int d\tau d\tau' \chi(\tau) \chi(\tau') W_D^{(2)}(x(\tau), x'(\tau')) e^{i\Omega(\tau - \tau')}. \quad (18)$$

Here, $W_D^{(2)}(x(\tau), x'(\tau'))$ is the D dimensional two point correlator (Wightman function). The exact functional form of the Wightman function again depends upon the background gravity.

We can consider more general interaction Hamiltonian,

$$\mathcal{H}_I = \lambda \chi_{\mathcal{T}}(\tau) m(\tau) \mathcal{O}_{\Phi}[x(\tau)], \quad (19)$$

Here, $m(\tau)$ the monopole operator,

$$m(\tau) = e^{i\Omega\tau} |e\rangle \langle g| + e^{-i\Omega\tau} |g\rangle \langle e| = \begin{pmatrix} 0 & e^{+i\Omega\tau} \\ e^{-i\Omega\tau} & 0 \end{pmatrix}. \quad (20)$$

This actually takes the ground state of the detector to the excited state and vice versa. In other words we can physically describe the procedure as "a click" in response to the presence of the field. Now the the operator \mathcal{O}_{Φ} outlines how the matter field is coupled to the detector. Instead of usual linear coupling we take a more general coupling²,

$$\mathcal{O}_{\Phi}[x(\tau)] = \Phi^n[x(\tau)] \quad (21)$$

²normal ordering is assumed

If we use the interaction Hamiltonian (21) then we re-express eq. (18),

$$\mathcal{P}_{g \rightarrow e}^{(2)} = \lambda^2 \int d\tau d\tau' \chi(\tau) \chi(\tau') W_D^{(2n)}(x(\tau), x'(\tau')) e^{i\Omega(\tau - \tau')} \quad (22)$$

Here, $W_D^{(2n)}(\tau - \tau') = \langle 0 | : \Phi^n(x(\tau)) :: \Phi^n(x(\tau')) : | 0 \rangle$ is the $2n$ -point correlator. The detector response function of the UDW detector is directly proportional to the probability for the detector to transition from ground state to excited state. Using Lorentzian switching function eq. (8) the response function $\mathcal{F}^{(2n)}(\Omega, \mathcal{T})$ will be,

$$\mathcal{F}^{(n)}(\Omega, \mathcal{T}) = \frac{\pi \mathcal{T}^3}{4} \int_{-\infty}^{\infty} d(\Delta\tau) \frac{W_D^{(n)}(\Delta\tau)}{\Delta\tau^2 + \mathcal{T}^2} e^{-i\Omega\Delta\tau} \quad (23)$$

The $2n$ -point function $W_D^{(2n)}(x, x')$ is related to the the Wightman function in the following interesting but simple way by Wick's theorem [29],

$$W_D^{(2n)}(x, x') = (n!) (W_D^{(2)}(x, x'))^n. \quad (24)$$

1.1 Finite time response of scalar fields: AdS spacetime

For conformally coupled scalars the Wightman function in $D > 2$ dimensional AdS spacetime can be obtained in the following form with suitable boundary condition[6],

$$W_{\text{AdS}_D}^{(2)}(x, x') = \langle 0 | \Phi(x(\tau)) \Phi(x(\tau')) | 0 \rangle = \mathcal{C}_D \left(\frac{1}{(v-1)^{D/2-1}} - \frac{1}{(v+1)^{D/2-1}} \right). \quad (25)$$

Here, ν is the conformal invariant defined as,

$$v = \frac{z^2 + z'^2 + (\mathbf{x} - \mathbf{x}')^2 - (t - t' - i\epsilon)^2}{2zz'}. \quad (26)$$

\mathcal{C}_D is a constant,

$$\mathcal{C}_D = \frac{k^{D-2} \Gamma(D/2 - 1)}{2(2\pi)^{D/2}}, \quad (27)$$

In this article we mainly focus on Unruh effect is a widely studied phenomena which basically states an accelerating observer (with constant linear acceleration a) will observe a thermal bath with temperature T . If the observer were in flat spacetime, the temperature is given by the following formula $T = \frac{\hbar a}{2\pi c k_B}$. In the usual literature[30] (studies mostly done in flat spacetime) the path which was chosen for the accelerating observer had linear uniform acceleration a . The accelerating observer (detector) can take a circular path with constant velocity v , will end up having constant acceleration a . Of course the resultant radiation (detector response) due to this type of non-linear motion will not be quite thermal radiation as the correlators will not obey the KMS relation [31]. We are interested in those accelerated paths which corresponds to Wightman function maintaining valid KMS relation.

1.1.1 Super critical accelerated paths in AdS

We are considering the supercritical paths ($a > k$) as only these paths results in non zero response function for the detectors[6] in uniform linear acceleration. In our recent article[23] we successfully showed that using GEMS (Global Embedding Minkowski Spacetimes) approach that one can construct a path with constant acceleration by considering the path as an intersection between a

flat plane of dimension M and D dimensional AdS hypersurface embedded in $D + 1$ dimensional flat spacetime. Here, $M(M < D + 1)$. We also proved that for any uniform linear supercritical trajectories would have the same conformal invariant v as a function of proper time.

$$v(\tau, \tau') = \frac{a^2}{\omega^2} - \frac{k^2}{\omega^2} \cosh(\omega(\tau - \tau') - i\epsilon). \quad (28)$$

Here $\omega = \sqrt{a^2 - k^2}$. The example of super critical path (with constant linear acceleration) in $z - t$ plane is given in ref. [23],

$$t(\tau) = \frac{a}{\omega} e^{\omega\tau}, \quad z(\tau) = e^{\omega\tau}, \quad x^1 = x^2 = x^3 = \dots = x^{D-2} = 0. \quad (29)$$

Another supercritical path with constant acceleration a in the $x_1 - t$ plane is given by the following manner[23],

$$z(\tau) = z_0, \quad x^1(\tau) = \frac{z_0 k}{\omega} \cosh(\omega\tau), \quad t(\tau) = \frac{z_0 k}{\omega} \sinh(\omega\tau), \quad x^2 = x^3 = \dots = x^{D-2} = 0. \quad (30)$$

z_0 is a constant and τ is the proper time. We could also define the (30) path in the $x^i - t$ direction. However we have already showed in ref.[23] that how all uniform accelerating paths with constant acceleration are related by AdS isometries. Any supercritical path will result in eq. (28). Therefore, following eq. (25), the two point function for uniform acceleration (in any supercritical path) becomes,

$$G_{\text{AdS}_D}(\Delta\tau) = \frac{\omega^{D-2} \Gamma(\frac{D}{2} - 1)}{(4\pi)^{\frac{D}{2}}} \left(\frac{1}{i^{D-2} \sinh^{D-2}(\frac{\omega\Delta\tau}{2} - i\epsilon)} - \frac{1}{(\sinh(A + (\frac{\omega\Delta\tau}{2} - i\epsilon)))^{\frac{D}{2}-1} (\sinh(A - (\frac{\omega\Delta\tau}{2} - i\epsilon)))^{\frac{D}{2}-1}} \right). \quad (31)$$

Here, $\sinh A = \omega/k$.

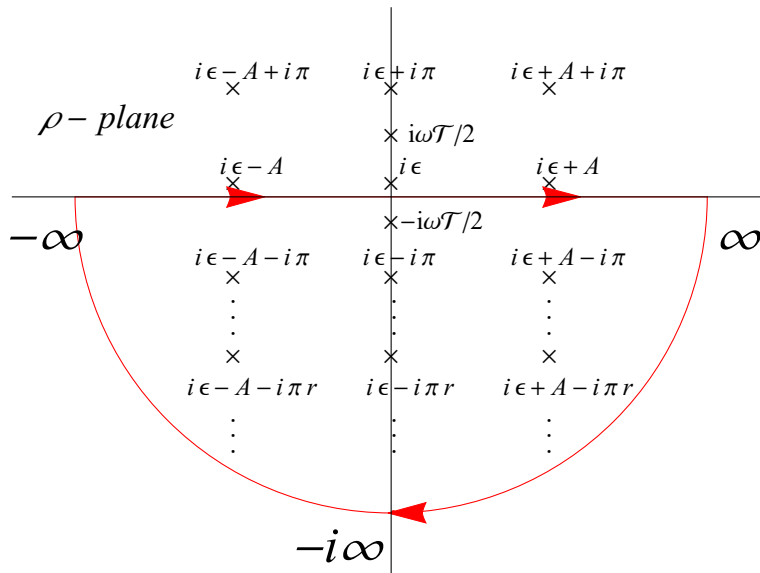


Figure 1: Contour for evaluating $I_{D,n,\alpha}$.

In our previous article we demonstrated the following relation about the two-point correlator[23],

$$W_{AdS_D}^{(2n)}\left(\Delta\tau + \frac{2\pi i}{\omega}\right) = (-1)^{nD} W_{AdS_D}^{(2n)}(\Delta\tau). \quad (32)$$

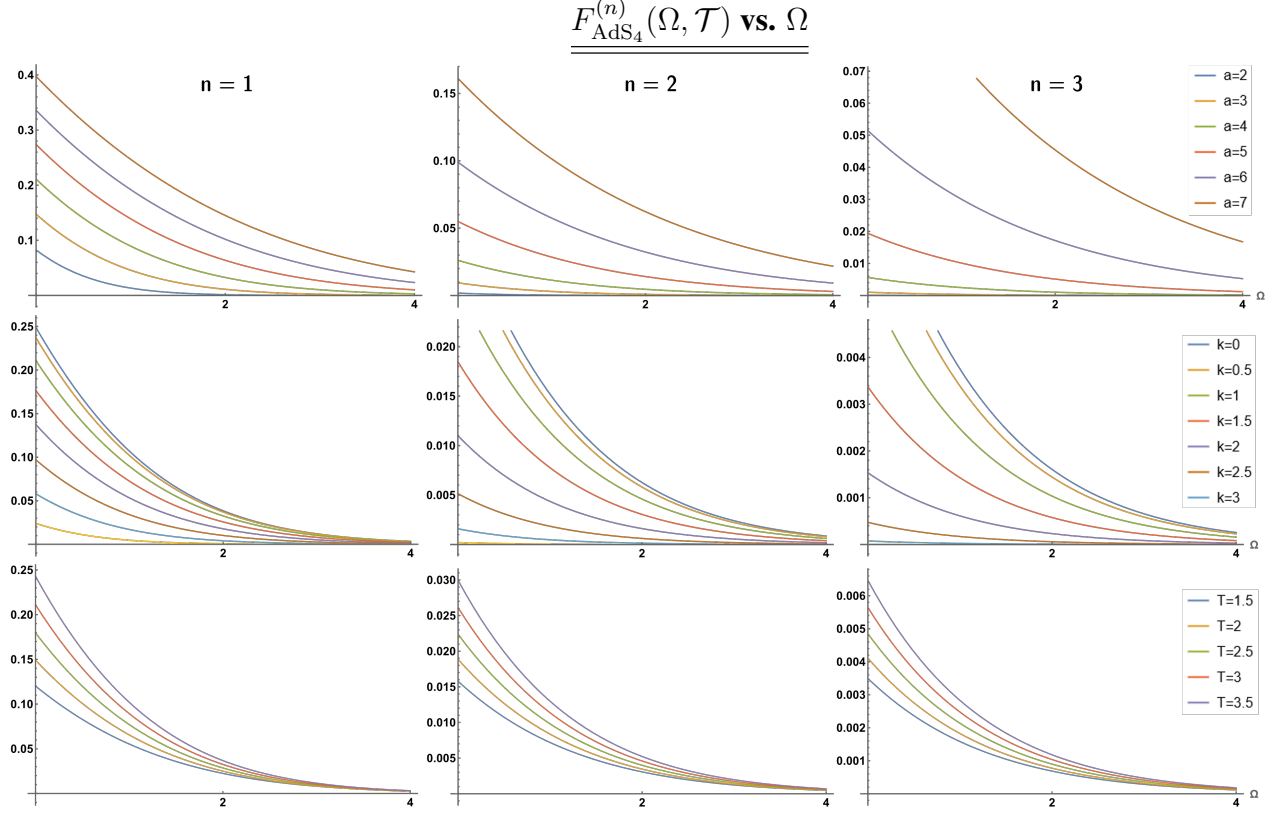


Figure 2: Plot of the finite-time response of the UDW particle detector in AdS Space-time against energy Ω . (From left to right) 1st, 2nd and 3rd columns show the plots for different values of n , with $n = 1$, $n = 2$ and $n = 3$. Each row (from top to bottom) shows the variation of the response function with changing a (fixed $k = 1$, $\mathcal{T} = 3$), changing k (fixed $a = 4$, $\mathcal{T} = 3$) and changing \mathcal{T} (fixed $a = 4$, $k = 1$) respectively.

Therefore $\omega = \sqrt{a^2 - k^2}$ is the temperature[23]. We rewrite the $2n$ -point function $G_{AdS_D}^{(n)}$ in the following manner [23],

$$G_{AdS_D}^{(n)}(\Delta\tau) = (n!) \mathcal{C}_D^n \left(\frac{\omega}{\sqrt{2k}}\right)^{n(D-2)} \sum_{\alpha=0}^n \binom{n}{\alpha} \frac{(-1)^\alpha}{i^p} \mathcal{G}_{D,n,\alpha}(\rho) \quad (33)$$

where,

$$\mathcal{G}_{D,n,\alpha}(\rho) = (\sinh(\rho - i\epsilon))^{-p} (\sinh(A + (\rho - i\epsilon)))^{-q} (\sinh(A - (\rho - i\epsilon)))^{-q} \quad (34)$$

$$\rho = \omega \Delta\tau / 2 \quad (35)$$

$$p = 2(n - \alpha)(D/2 - 1) \quad (36)$$

$$q = \alpha(D/2 - 1). \quad (37)$$

So, finally the expression for the finite time response function in AdS spacetime for our interaction

Hamiltonian becomes,

$$\mathcal{F}^{(n)}(\Omega, \mathcal{T}) = \frac{\pi n! \mathcal{T}^3 C_D^n}{4} \left(\frac{\omega}{\sqrt{2k}} \right)^{n(D-2)} \int_{-\infty}^{\infty} d(\Delta\tau) \frac{e^{-i\Omega\Delta\tau}}{\Delta\tau^2 + \mathcal{T}^2} \sum_{\alpha=0}^n \binom{n}{\alpha} \frac{(-1)^\alpha}{i^p} \mathcal{G}_{D,n,\alpha}(\rho) \quad (38)$$

$$= \frac{\pi n! \mathcal{T}^3 C_D^n}{4} \left(\frac{\omega}{\sqrt{2k}} \right)^{n(D-2)} \sum_{\alpha=0}^n \binom{n}{\alpha} \frac{(-1)^\alpha}{i^p} \left(\frac{\omega}{2} \right) \underbrace{\int_{-\infty}^{\infty} d\rho \frac{e^{-i(2\Omega/\omega)\rho}}{\rho^2 + (\omega\mathcal{T}/2)^2} \mathcal{G}_{D,n,\alpha}(\rho)}_{\mathcal{F}_{D,n,\alpha}} \quad (39)$$

$$= \frac{\omega \pi n! \mathcal{T}^3 C_D^n}{8} \left(\frac{\omega}{\sqrt{2k}} \right)^{n(D-2)} \sum_{\alpha=0}^n \binom{n}{\alpha} \frac{(-1)^\alpha}{i^p} \mathcal{F}_{D,n,\alpha} \quad (41)$$

where,

$$\mathcal{F}_{D,n,\alpha} = \int_{-\infty}^{\infty} d\rho \frac{e^{-i(2\Omega/\omega)\rho}}{\rho^2 + (\omega\mathcal{T}/2)^2} \mathcal{G}_{D,n,\alpha}(\rho). \quad (42)$$

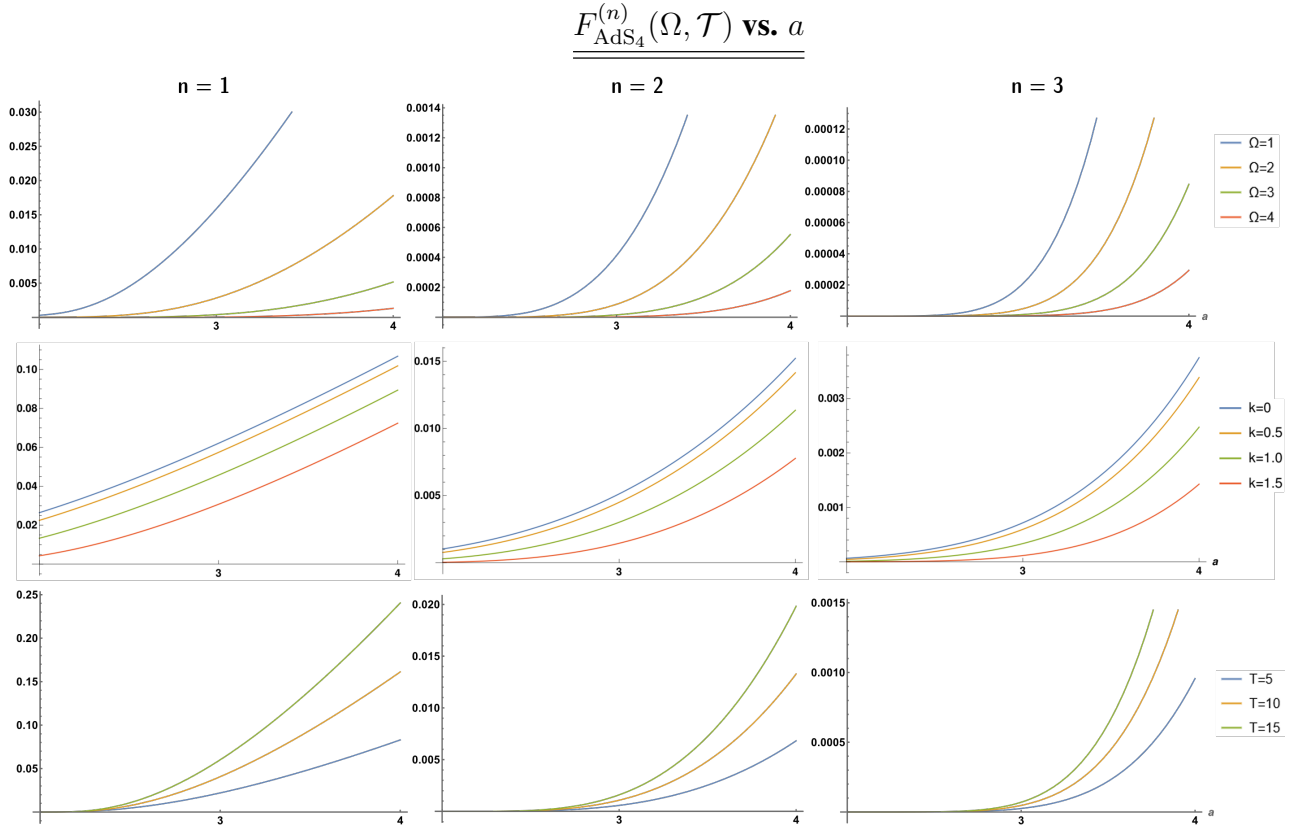


Figure 3: Plot of the Finite-Time response of the UDW Particle detector in AdS Space-time against acceleration a . (From left to right) 1st, 2nd and 3rd columns show the plots for different values of n , with $n = 1$, $n = 2$ and $n = 3$, respectively. Each row (from top to bottom) shows the variation of the response function with changing Ω (fixed $k = 2$, $\mathcal{T} = 3$), changing k ($\Omega = 1$, $\mathcal{T} = 3$) and changing \mathcal{T} ($\Omega = 1$, $k = 2$) respectively.

Next, we evaluate $\mathcal{F}_{D,n,\alpha}$ by computing the contour integral using semi-circle contour containing the lower half of complex ρ plane (shown in Fig. 1). Thus we obtain,

$$\begin{aligned}
\mathcal{F}_{D,n,\alpha}(\mathcal{T}) &= -2\pi i \times \left\{ \text{sum of the residues at } \rho = -i\pi r, \pm A - i\pi r \text{ (where } r = 1, 2, \dots) \right. \\
&\quad \left. \text{and } \rho = -i\omega\mathcal{T}/2 \text{ of } \frac{\mathcal{G}_{D,n,\alpha}(\rho)}{\rho^2 + (\omega\mathcal{T}/2)^2} \right\} \\
&= -2\pi i \times \left(\lim_{\rho \rightarrow -i\omega\mathcal{T}/2} \frac{e^{-i(2\Omega/\omega)\rho}}{\sinh^q(A+\rho) \sinh^q(A-\rho) \sinh^p(\rho) \left(\rho - \left(\frac{i\omega\mathcal{T}}{2}\right)\right)} + \right. \\
&\quad \sum_{r=1}^{\infty} \left[\lim_{\rho \rightarrow -i\pi r - A} \frac{\eta(q-1)}{\Gamma(q)} \left(\frac{1}{\cosh(\rho+A)} \frac{d}{d\rho} \right)^{q-1} \frac{e^{-i(2\Omega/\omega)\rho}}{\cosh(A+\rho) \sinh^q(A-\rho) \sinh^p(\rho) \left(\rho^2 + \left(\frac{\omega\mathcal{T}}{2}\right)^2\right)} + \right. \\
&\quad \left. \lim_{\rho \rightarrow -i\pi r + A} \frac{\eta(q-1)}{\Gamma(q)} \left(\frac{-1}{\cosh(A-\rho)} \frac{d}{d\rho} \right)^{q-1} \frac{-e^{-i(2\Omega/\omega)\rho}}{\sinh^q(A+\rho) \cosh(A-\rho) \sinh^p(\rho) \left(\rho^2 + \left(\frac{\omega\mathcal{T}}{2}\right)^2\right)} + \right. \\
&\quad \left. \left. \lim_{\rho \rightarrow -i\pi r} \frac{\eta(p-1)}{\Gamma(p)} \left(\frac{1}{\cosh \rho} \frac{d}{d\rho} \right)^{p-1} \frac{e^{-i(2\Omega/\omega)\rho}}{\sinh^q(A+\rho) \sinh^q(A-\rho) \cosh(\rho) \left(\rho^2 + \left(\frac{\omega\mathcal{T}}{2}\right)^2\right)} \right] \right) \quad (43)
\end{aligned}$$

Here, $\eta(p)$ is Heaviside step function and $\Gamma(p)$ is gamma function. In our previous case we were able to analytically solve the four dimensional response function in AdS when we chose the infinite switching time, i.e. $\mathcal{T} = \infty$. However it was not possible to calculate the detector response for finite switching time. We have evaluated the response function numerically in finite switching time. Finally we have plotted the response function in different ranges of parameter space. In figure 2, we plot the detector response as a function of energy gap of the two level UdW detector. In the three different columns of figure 2, we have chosen three values of n . We can see that when the detector energy gap increases the response goes to zero. In the first row we have fixed the curvature and switching time while varying the energy. We can clearly see the response weakens with greater value of n . But if we increase the acceleration of the detector the temperature of the radiation also increases. Therefore the first row of Fig 2 manifests response function with respect to Ω takes greater value when acceleration is increased. Similar trends are noticed when we look at the other two plots of figure 1. It is very interesting to see as the curvature of AdS spacetime goes to zero the detector response rises. Complete opposite trends are noticed in dS spacetime. But in both cases we have better response function if we can "turn on" the detector for longer time.

As expected from previous discussion if we can accelerate the detectors more and more, we should be able have best response from the detector. We also see it in figure 3. In the first row of figure 3 we can notice when energy gap rises the response weakens. Even if the detector is accelerated with higher value it will be difficult to excite the detector if the energy gap is too much. This problem persists more if we have non-linear coupling between the matter field and the detector. The trend of response function changing with curvature is very interesting. As the curvature increases more and more it becomes problematic to excite the detector. However, we should point out AdS spacetime is a constant curvature spacetime. So when we plot for different values of k , we mean that we are comparing the results the results of response function for different AdS spacetime with different curvatures. We do not mean that we are analysing the detector spectrum where the gravitational background has varying curvature.

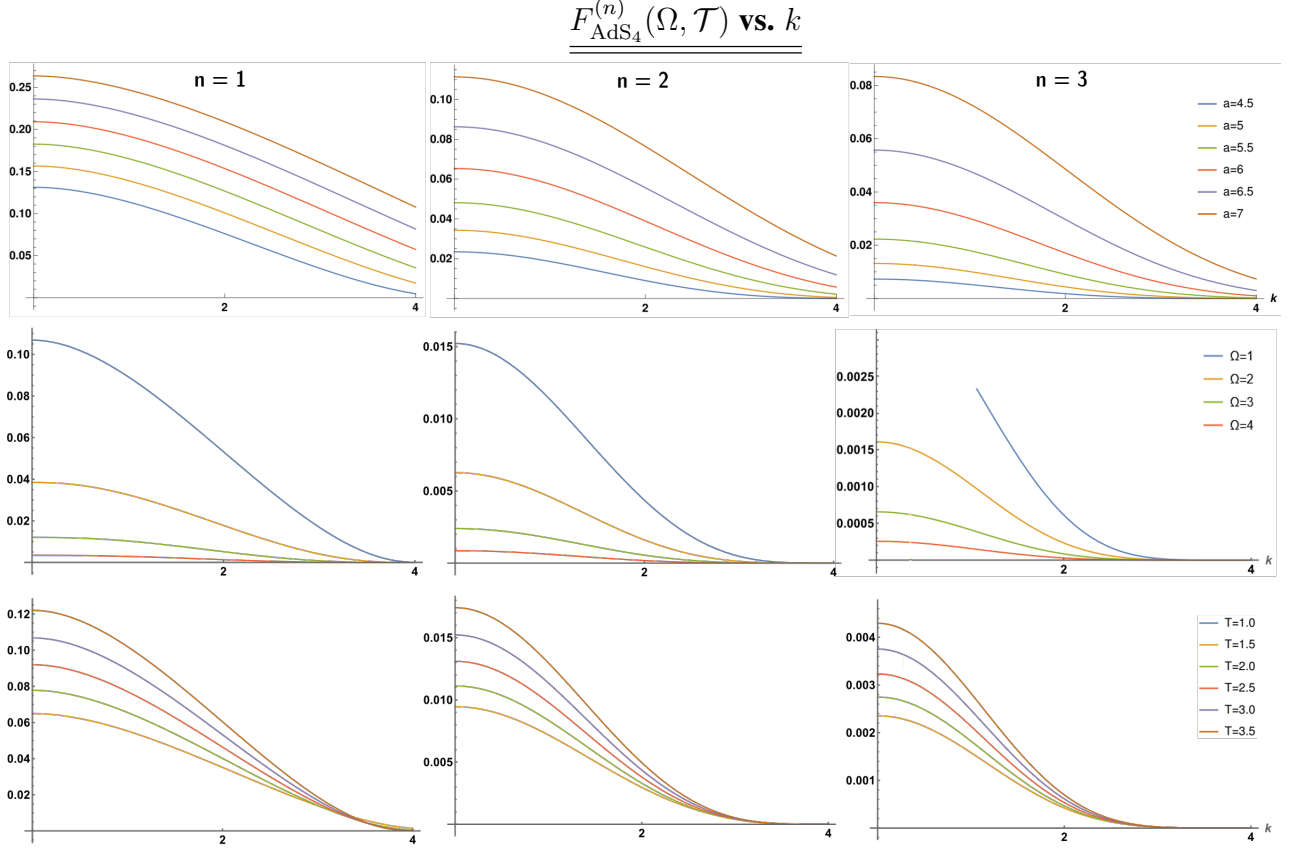


Figure 4: Plot of the Finite-Time response of the UDW Particle Detector in AdS Space-time against the curvature of AdS (k) for massless scalar fields. (From left to right) 1st, 2nd and 3rd columns show the plots for the $n = 1$, $n = 2$ and $n = 3$ coupling to the scalar field. Each row (from top to bottom) shows the variation of the response function with changing a ($\mathcal{T} = 3, \Omega = 1$), changing Ω ($a = 4, \mathcal{T} = 3$) and changing \mathcal{T} ($a = 4, \Omega = 1$) respectively.

1.2 Scalar field in dS space

We now we use the same setup of two level detector as before but now we consider that the background spacetime is de Sitter spacetime. The metric of de Sitter spacetime can be expressed by so called flat slicing as below-

$$ds^2 = \frac{1}{k^2 \eta^2} (d\eta^2 - dx_1^2 - dx_2^2 - \dots - dx_{D-1}^2). \quad (44)$$

Now, we are going to discuss about the real scalar field Φ that is conformally coupled to dS gravitational background. We have the same matter field action as well as the same interaction Hamiltonian as in previous section (eq. (19)). Just as before we need to know the two-point correlator (Wightman function) in order to evaluate the detector response. The Wightman function for "Euclidean" vacuum $|0\rangle$ can easily be obtained for conformally coupled real scalar field [32, 31],

$$W_{\text{dSD}}^{(2)}(x, x') = \langle 0 | \Phi(x(\eta)) \Phi(x(\eta')) | 0 \rangle = \mathcal{K}_D v^{1-D/2} \quad (45)$$

where,

$$\mathcal{K}_D = \frac{k^{D-2} \Gamma(D/2 - 1)}{2(2\pi)^{D/2}}. \quad (46)$$

Here ν is the conformal invariant.

$$\nu = \frac{(\vec{x} - \vec{x}')^2 - (\eta - \eta' - i\epsilon)^2}{2\eta\eta'}. \quad (47)$$

In order to examine Unruh radiation through the detectors need to move through a constant accelerated path in dS background. An example of accelerating path in dS spacetime with constant linear acceleration (see Appendix 5), we can choose the following,

$$\eta(\tau) = \tau_0 e^{\omega\tau}, \quad x^1(\tau) = \frac{a}{\omega} \tau_0 e^{\omega\tau}, \quad x^2 = x^3 = \dots = x^{D-1} = 0, \quad (48)$$

where $\omega = \sqrt{a^2 + k^2}$. Plugging η and x^i from eq. (48) to eq. (47), the conformal invariant ν takes the following form in this case,

$$\begin{aligned} \nu &= \frac{(\frac{a}{\omega} \tau_0 e^{\omega\tau} - \frac{a}{\omega} \tau_0 e^{\omega\tau'})^2 - (\tau_0 e^{\omega\tau} - \tau_0 e^{\omega\tau'})^2}{2\tau_0^2 e^{\omega\tau} e^{\omega\tau'}} \\ &= \frac{1}{2} \left(\frac{a^2}{\omega^2} - 1 \right) \left(\frac{e^{\omega\tau} - e^{\omega\tau'}}{e^{\omega(\tau+\tau')/2}} \right)^2 \\ &= -\frac{H^2}{2\omega^2} \left(e^{\omega\Delta\tau/2} - e^{-\omega\Delta\tau/2} \right)^2 \\ &= -\frac{2H^2}{\omega^2} \sinh^2(\omega\Delta\tau/2) \end{aligned} \quad (49)$$

Following eq. (45), the two point function for uniformly accelerating paths becomes,

$$G_{\text{dS}_D}(\Delta\tau) = \frac{\omega^{D-2} \Gamma(\frac{D}{2} - 1)}{(4\pi)^{\frac{D}{2}}} \frac{1}{i^{D-2} \sinh^{D-2}(\omega\Delta\tau/2 - i\epsilon)}. \quad (50)$$

We can define the transition probability rate or detector's response function (per unit time)³ for interaction Lagrangian (7) of scalars[27],

$$\mathcal{F}_{\text{dS}_D}^{(n)} = \int_{-\infty}^{\infty} d\Delta\tau e^{-iE\Delta\tau} W_{\text{dS}_D}^{(2n)}(\Delta\tau). \quad (51)$$

Here, $W_{\text{dS}_D}^{(2n)}(\tau - \tau') = \langle 0 | : \Phi^n(x(\tau)) :: \Phi^n(x(\tau')) : | 0 \rangle$ is the $2n$ correlator. The $2n$ -point function $W_{\text{dS}_D}^{(2n)}$ is related to the the Wightman function in the following way by Wick's theorem [29],

$$W_{\text{dS}_D}^{(2n)}(x, x') = (n!) \left(W_{\text{dS}_D}^{(2)}(x, x') \right)^n. \quad (52)$$

So, the $2n$ correlator becomes,

$$W_{\text{dS}_D}^{(2n)}(\Delta\tau) = (n!) \mathcal{K}_D^n \left(\frac{\omega}{\sqrt{2H}} \right)^{n(D-2)} \left(\frac{1}{i^{D-2} \sinh^{D-2}(\frac{\omega\Delta\tau}{2} - i\epsilon)} \right)^n. \quad (53)$$

Now the KMS condition can be easily checked using the equation (53).

$$\begin{aligned} W_{\text{dS}_D}^{(2n)}(\Delta\tau + \frac{2\pi i}{\omega}) &= (n!) \mathcal{K}_D^n \left(\frac{\omega}{\sqrt{2H}} \right)^{n(D-2)} \left(\frac{1}{i^{D-2} \sinh^{D-2}(\frac{\omega}{2}(\Delta\tau + \frac{2\pi i}{\omega}) - i\epsilon)} \right)^n \\ &= (-1)^{nD} W_{\text{dS}_D}^{(2n)}(\Delta\tau). \end{aligned} \quad (54)$$

³In this scenario, we are considering the detector can be switched on for infinite time.

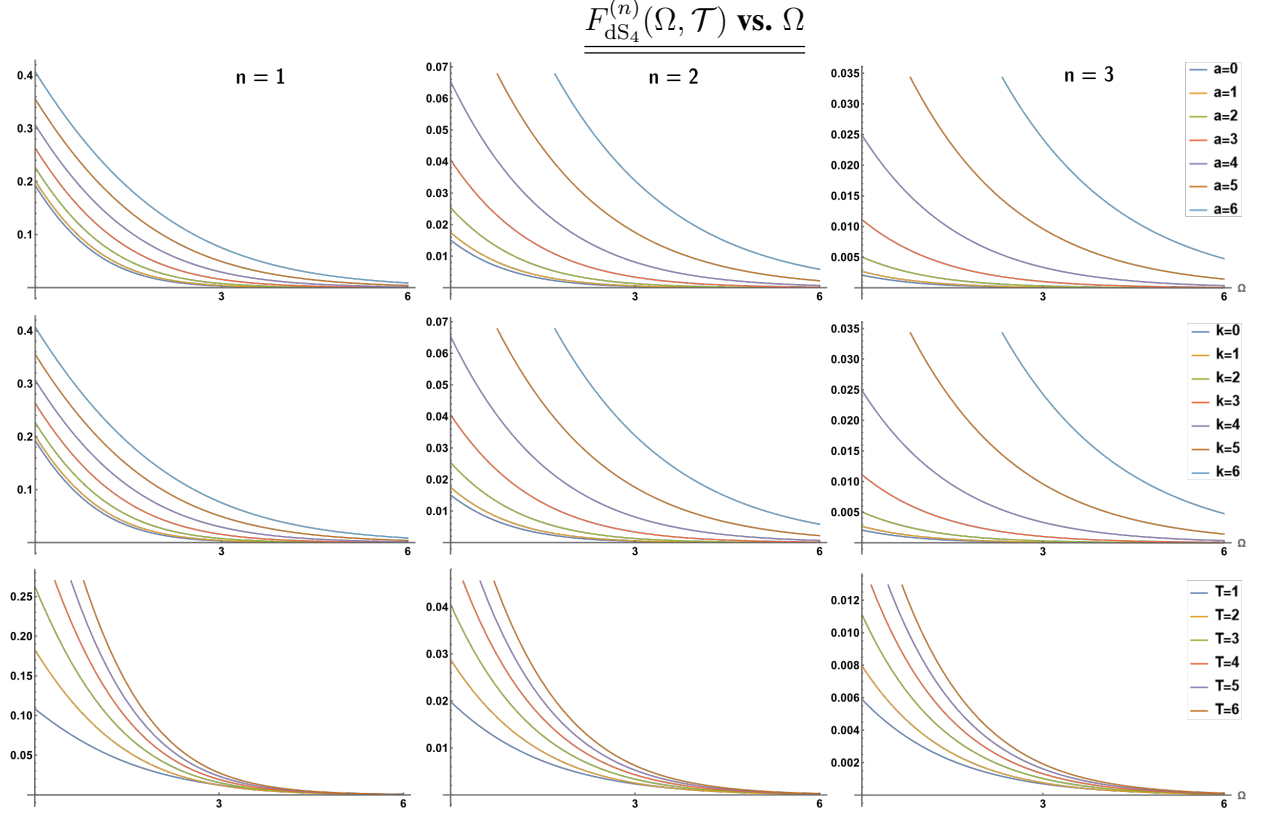


Figure 5: Plot of the finite-time response of the UDW particle detector in dS space-time against energy Ω . (From left to right) 1st, 2nd and 3rd columns show the plots for different values of n , with $n = 1$, $n = 2$ and $n = 3$. Each row (from top to bottom) shows the variation of the response function with changing a (fixed $k = 3$, $\mathcal{T} = 3$), changing k (fixed $a = 3$, $\mathcal{T} = 3$) and changing \mathcal{T} (fixed $a = 3$, $k = 3$) respectively.

This behavior is similar to the AdS space for nonlinear coupling [33] with a major difference with radiation temperature being $\omega = \sqrt{a^2 + k^2}$ [3]. We can obtain the Unruh-Dewitt detector response function by taking $\alpha \rightarrow 0$ in equation (37) in [33].

$$\mathcal{F}_{dS_D}^{(n)} = \left(n! \mathcal{K}_D^n \left(\frac{\omega}{\sqrt{2}H} \right)^{n(D-2)} \frac{(-1)^{n(D-2)+1}}{i^{n(D-2)}} \frac{2}{\omega} I_{D,n} \right) \frac{1}{e^{2\pi E/\omega} - (-1)^{n(D-2)}}. \quad (55)$$

where,

$$I_{D,n} = 2\pi i \times \frac{1}{\Gamma(n(D-2))} \lim_{\rho \rightarrow 0} \left(\left(\frac{1}{\cosh \rho} \frac{d}{d\rho} \right)^{n(D-2)-1} \frac{e^{-i\frac{2E}{\omega}\rho}}{\cosh(\rho)} \right). \quad (56)$$

Finally, to calculate the finite-time Unruh-DeWitt detector response function for dS spacetime, we

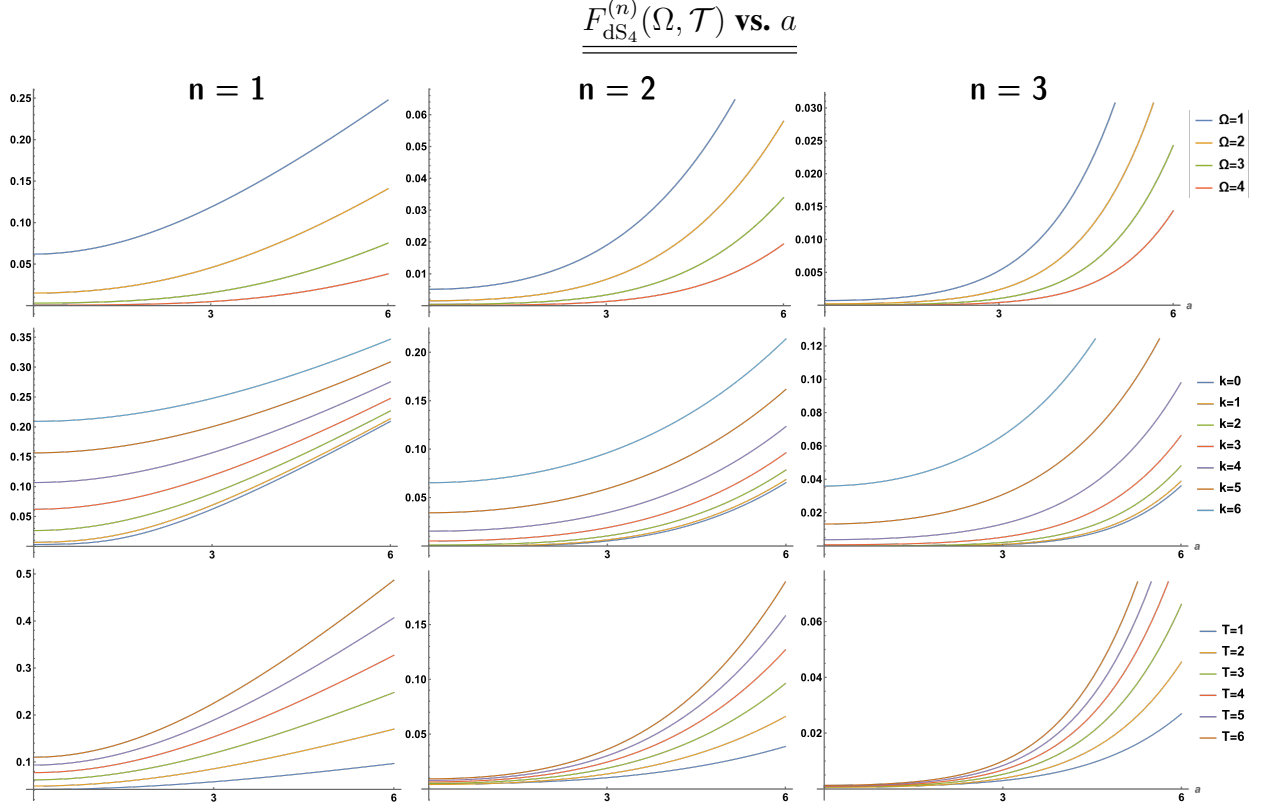


Figure 6: Plot of the Finite-Time response of the UDW Particle detector in dS Space-time against acceleration a . (From left to right) 1st, 2nd and 3rd columns show the plots for different values of n , with $n = 1$, $n = 2$ and $n = 3$. Each row (from top to bottom) shows the variation of the response function with changing Ω (fixed $k = 3$, $\mathcal{T} = 3$), changing k ($\Omega = 1$, $\mathcal{T} = 3$) and changing \mathcal{T} ($\Omega = 1$, $k = 3$) respectively.

plug in the 2n-point correlator $G_{\text{dS}_D}^{(n)}$ from eq. (53) to eq. (51) which gives,

$$\begin{aligned}
\mathcal{F}_{\text{dS}_D}^{(n)}(\Omega, \mathcal{T}) &= \frac{\pi \mathcal{T}^3}{4} \int_{-\infty}^{\infty} d(\Delta\tau) \frac{G_{\text{dS}_D}^{(n)}(\Delta\tau)}{\Delta\tau^2 + \mathcal{T}^2} e^{-i\Omega\Delta\tau} \\
&= \frac{\pi \mathcal{T}^3 n!}{4} \left(\frac{\Gamma(D/2 - 1)}{(4\pi)^{D/2}} \right)^n \left(\frac{\omega}{i} \right)^{n(D-2)} \int_{-\infty}^{\infty} d(\Delta\tau) \frac{e^{-i\Omega\Delta\tau}}{\Delta\tau^2 + \mathcal{T}^2} \frac{1}{\sinh^{n(D-2)}\left(\frac{\omega\Delta\tau}{2} - i\epsilon\right)} \\
&= \frac{\pi \mathcal{T}^3 n!}{4} \left(\frac{\Gamma(D/2 - 1)}{(4\pi)^{D/2}} \right)^n \left(\frac{\omega}{i} \right)^{n(D-2)} \left(\frac{\omega}{2} \right) \underbrace{\int_{-\infty}^{\infty} d\rho \frac{e^{-2i\Omega\rho/\omega}}{\rho^2 + (\omega\mathcal{T}/2)^2} \frac{1}{\sinh^{n(D-2)}(\rho - i\epsilon)}}_{\mathcal{F}_{D,n}} \\
&= \frac{\pi \mathcal{T}^3 n!}{4} \left(\frac{\Gamma(D/2 - 1)}{(4\pi)^{D/2}} \right)^n \left(\frac{\omega}{i} \right)^{n(D-2)} \left(\frac{\omega}{2} \right) \cdot \mathcal{F}_{D,n} \tag{57}
\end{aligned}$$

where,

$$\mathcal{F}_{D,n} = \int_{-\infty}^{\infty} d\rho \frac{e^{-2i\Omega\rho/\omega}}{\rho^2 + (\omega\mathcal{T}/2)^2} \frac{1}{\sinh^{n(D-2)}(\rho - i\epsilon)} \tag{58}$$

Finally, we evaluate the finite time response function $\mathcal{F}_{\text{dS}_D}^{(n)}$ numerically from (57) and plot it with respect to energy gap, acceleration, and curvature as before. Just like the case of AdS, we can also

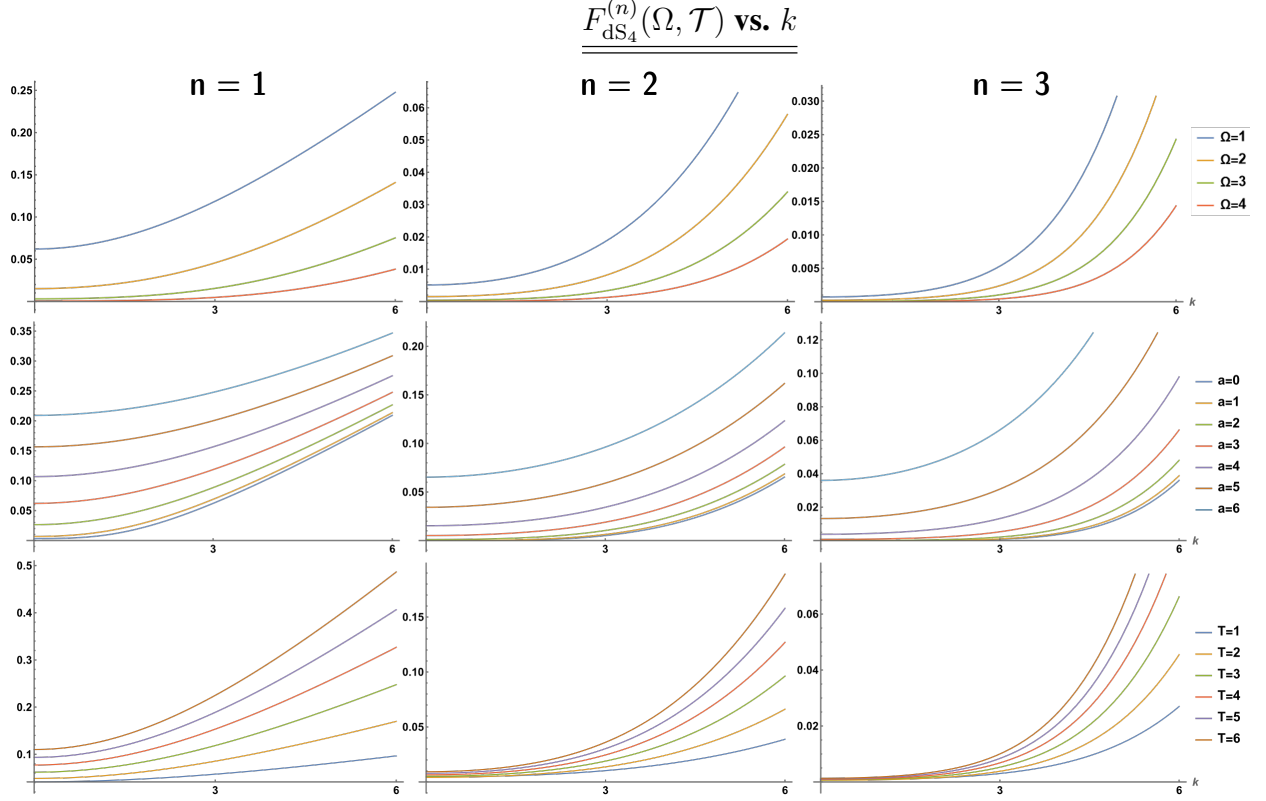


Figure 7: Plot of the Finite-Time response of the UDW Particle Detector in dS Space-time against the curvature of space-time (k) for massless scalar fields. (From left to right) 1st, 2nd and 3rd columns show the plots for different values of n , with $n = 1$, $n = 2$ and $n = 3$. Each row (from top to bottom) shows the variation of the response function with changing Ω ($a = 3, \mathcal{T} = 3$), changing a ($\mathcal{T} = 3, \Omega = 1$), and changing \mathcal{T} ($a = 3, \Omega = 1$) respectively.

see that as the energy gap increases the response function decreases (Fig. 5). In the first row of figure 5 we can see if the value of acceleration is higher the response function.

2 Finite time response of UDW detector: Dirac fields.

2.1 Dirac fields in AdS

In the similar fashion we can analyse the response function for fermions in AdS spacetime minimally coupled to background gravity. The fermionic matter field action is-

$$\mathcal{S}_0 = \int d^D x \sqrt{|g|} \bar{\Psi} i \not{D} \Psi. \quad (59)$$

We can consider usual interaction Hamiltonian[20],

$$\mathcal{H}_{\text{Int}} = \lambda \chi_{\mathcal{T}}(\tau) m(\tau) \mathcal{O}_{\Psi}[x(\tau)], \quad (60)$$

Here, the operator $\mathcal{O}_{\Psi}[x(\tau)]$ is the normal ordered bispinor,

$$\mathcal{O}_{\Psi}[x(\tau)] =: \bar{\Psi}[x(\tau)] \Psi[x(\tau)] : \quad (61)$$

Using Lorentzian switching function eq. (8) the response function for interaction Hamiltonian (60) takes the following form,

$$\mathcal{F}^{(n)}(\Omega, \mathcal{T}) = \frac{\pi \mathcal{T}^3}{4} \int_{-\infty}^{\infty} d(\Delta\tau) \frac{S_D^{(4)}(\Delta\tau)}{\Delta\tau^2 + \mathcal{T}^2} e^{-i\Omega\Delta\tau}. \quad (62)$$

Here, the four point function $S_D^{(4)}$,

$$\begin{aligned} S_D^{(4)}(x(\tau), x(\tau')) &= \langle 0 | : (\bar{\Psi}_a(x(\tau))) \Psi_a(x(\tau)) :: (\bar{\Psi}_b(x(\tau'))) \Psi_b(x(\tau')) : | 0 \rangle \\ &= \text{Tr}[S^+(x, x') S^-(x', x)]. \end{aligned} \quad (63)$$

As discussed in [23] for fermions in AdS spacetime,

$$S_D^{(2)}(\Delta\tau) = N \frac{(\Gamma(D/2))^2}{\Gamma(D-1)} G_{AdS_{2D}}(\Delta\tau) \quad (64)$$

From eq. (100) we can then conclude that detector response function for fermions can be related to response function for the scalars,

$$\mathcal{J}_{AdS_D}(\Delta\tau) = N \frac{(\Gamma(D/2))^2}{\Gamma(D-1)} \mathcal{F}_{AdS_{2D}}^{(1)}(\Delta\tau). \quad (65)$$

In the next section we work on fermions in dS spacetime and we work out relations similar to eq. (64). Therefore, we further demonstrate that eq. (65) holds for maximally symmetric spacetime. The proof is similar to the case of AdS but we explicitly demonstrate it for the sake of completeness.

2.2 Dirac fields in dS

In order to study Dirac field in de Sitter spacetime we choose a local Lorentz frame (vielbein) which is defined as, $e_\mu^a = \delta_\mu^a / (H\tau)$ such that $g_{\mu\nu} = e_\mu^a e_\nu^b \eta_{ab}$ mimics the de-Sitter metric. Here Latin letters a, b corresponds to local orthonormal flat coordinates and Greek letters μ, ν signifies the de Sitter coordinates. Both of them takes value from 0 to $D-1$. Also $\eta_{ab} = \text{diag}(+1, -1, \dots, -1)$ is the local flat metric. The vielbeins follow the usual orthonormal relations. Now, the curved space Γ matrices and the covariant derivatives are defined as,

$$\begin{aligned} \Gamma^\mu &= e_\mu^a \gamma^a, \\ D_\mu &= \partial_\mu + \frac{1}{2} \omega_\mu^{bc} \Omega_{bc}, \end{aligned} \quad (66)$$

where γ_a are gamma matrices in flat spacetime. And commutator between γ matrices are identified as Ω_{bc} .

$$\Omega^{bc} = \frac{1}{4} [\gamma^b, \gamma^c] \quad (67)$$

and the spin connections ω_μ^{bc} are noted as,

$$\omega_\mu^{ab} = e^{a\lambda} (\partial_\mu e_\lambda^b - \left\{ \begin{matrix} \alpha \\ \mu \lambda \end{matrix} \right\} e_\alpha^b) \quad (68)$$

and $\left\{ \begin{matrix} \alpha \\ \mu \lambda \end{matrix} \right\}$ are the Christoffel symbols related to dS spacetime metric eq. (1). Here Γ^μ and γ^a maintain the well-known Clifford algebra,

$$\begin{aligned} \{\Gamma^\mu, \Gamma^\nu\} &= 2g^{\mu\nu} \mathbb{I}_{N \times N} \\ \{\gamma^b, \gamma^c\} &= 2\eta^{bc} \mathbb{I}_{N \times N}. \end{aligned} \quad (69)$$

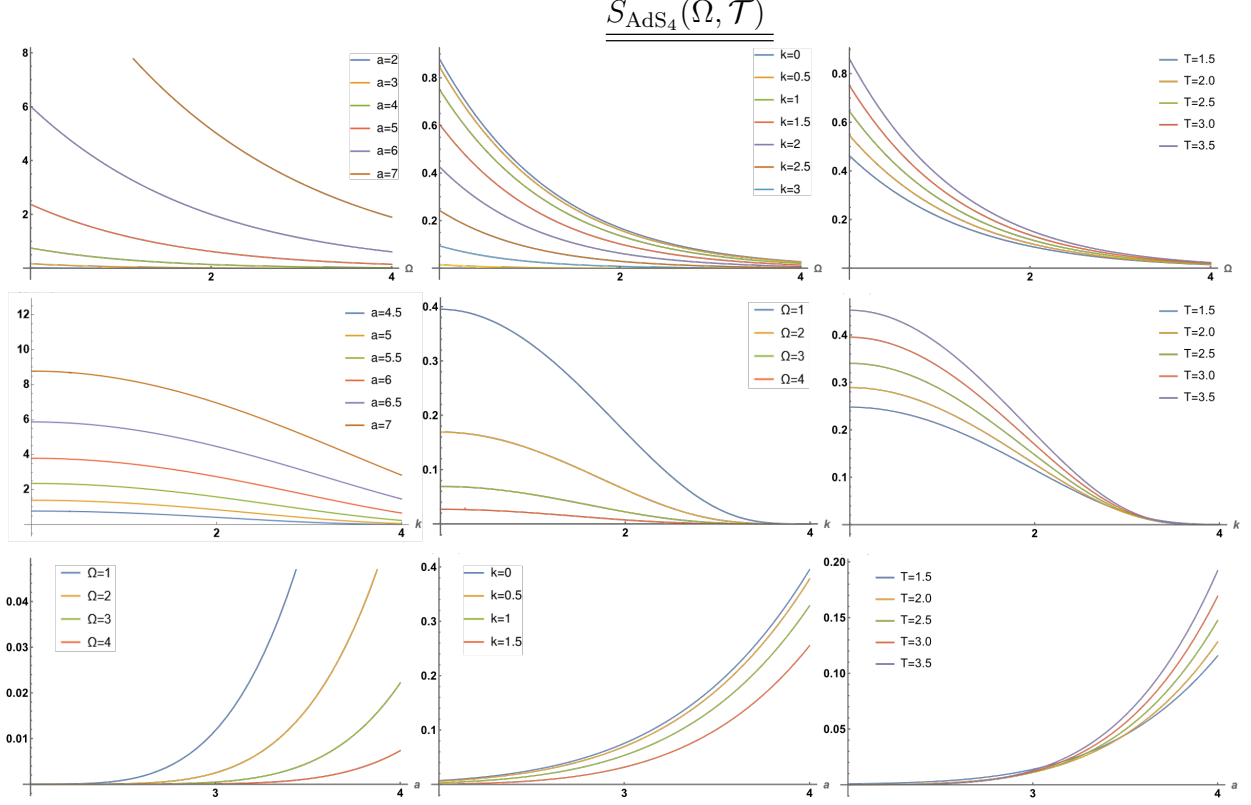


Figure 8: Plot of the Finite-Time response of the UDW Particle Detector in AdS Space-time coupled to a fermionic Field. Each row (from top to bottom) shows the plot of the response function against Ω (varying $a[\mathcal{T} = 3, k = 1]$, varying $k[\mathcal{T} = 3, a = 4]$ and varying $\mathcal{T}[a = 4, k = 1]$), against k (varying $a[\Omega = 1, \mathcal{T} = 3]$, varying $\Omega[a = 4, \mathcal{T} = 3]$ and varying $\mathcal{T}[a = 4, \Omega = 1]$), and against a (varying $\Omega[k = 2, \mathcal{T} = 3]$, varying $k[\Omega = 1, \mathcal{T} = 3]$ and varying $\mathcal{T}[k = 2, \Omega = 1]$) respectively.

with,

$$N = \begin{cases} 2^{\frac{D}{2}} & D \text{ is even} \\ 2^{\frac{D-1}{2}} & D \text{ is odd.} \end{cases} \quad (70)$$

In dS spacetime, the Dirac operator takes the form,

$$\mathcal{D} = \Gamma^\mu D_\mu \equiv e_a^\mu \gamma^a \left(\partial_\mu + \frac{1}{2} \omega_\mu^{bc} \Omega_{bc} \right) = k\eta \left(\gamma^a \partial_a - \frac{D-1}{2\eta} \gamma^0 \right). \quad (71)$$

To derive this relation we used

$$\left\{ \begin{array}{c} \alpha \\ \mu \quad \lambda \end{array} \right\} = \frac{1}{\eta} (g^{\alpha 0} g_{\mu\lambda} - \delta_\lambda^\alpha \delta_\mu^0 - \delta_\mu^\alpha \delta_\lambda^0), \quad (72)$$

$$\omega_\mu^{ab} = \frac{g^{\beta 0}}{\eta} (e_\mu^b e_\beta^a - e_\mu^a e_\beta^b). \quad (73)$$

In dS spacetime minimally coupled Dirac fermions with mass m to background gravity will have the action,

$$\mathcal{S}_0 = \int d^D x \sqrt{|g|} (\bar{\Psi} i \mathcal{D} \Psi - m \bar{\Psi} \Psi). \quad (74)$$

We can split the Ψ field in two parts, namely positive and negative frequency modes.

$$\Psi(x) = \Psi^+(x) + \Psi^-(x). \quad (75)$$

These are the solution of massive Dirac equation derived from equation (74)

$$i\not{D}\Psi - m\Psi = 0. \quad (76)$$

We will first look into the positive energy mode solutions $\psi^{(+)}$ of (76). These solutions are proportional to $e^{i\mathbf{p}\mathbf{x}}$, where $\mathbf{x} = (x^1, \dots, x^{D-1})$ and $\mathbf{p} = (p_1, \dots, p_{D-1})$, $\mathbf{p}\mathbf{x} = p_l x^l$, and the summation runs over $l = 1, \dots, D - 1$. We now decompose the positive energy modes into upper and lower components,

$$\psi^{(+)} = \begin{bmatrix} \psi_+(\eta) \\ \psi_-(\eta) \end{bmatrix} e^{i\mathbf{p}\mathbf{x}}. \quad (77)$$

This can be done by using the following explicit definition Gamma matrix representation,

$$\gamma^0 = \begin{bmatrix} \mathbb{I}_{(N/2) \times (N/2)} & \mathbf{0}_{(N/2) \times (N/2)} \\ \mathbf{0}_{(N/2) \times (N/2)} & -\mathbb{I}_{(N/2) \times (N/2)} \end{bmatrix}, \quad \gamma^a = \begin{bmatrix} \mathbf{0}_{(N/2) \times (N/2)} & \sigma^a \\ -\sigma^a & \mathbf{0}_{(N/2) \times (N/2)} \end{bmatrix}, \quad (78)$$

with $a = 1, \dots, D - 1$. The definitions of $\mathbb{I}_{(N/2) \times (N/2)}$ and $\mathbf{0}_{(N/2) \times (N/2)}$ can be found in [23].

$$\begin{aligned} \sigma^a \sigma^b + \sigma^b \sigma^a &= 2\delta^{ab} \mathbb{I}_{(N/2) \times (N/2)}, \\ \sigma^{a\dagger} &= \sigma^a. \end{aligned}$$

The Dirac equation is then reduced to subsequent form for positive energy modes,

$$\left(\partial_0 - \frac{D-1}{2\eta} \pm \frac{im}{k\eta} \psi_{\pm} \right) - ip_l \sigma^l \psi_{\mp} = 0. \quad (79)$$

Using equation (79) we can deduce two different second order differential equations for the upper and lower components:

$$\left(\eta^2 \partial_0^2 - (D-1)\eta \partial_0 + p^2 \eta^2 + \frac{(D-1)^2}{4} + \frac{D-1}{2} + \frac{m^2}{H^2} \mp \frac{im}{k} \right) \psi_{\pm} = 0. \quad (80)$$

Making the following substitution,

$$\psi_{\pm}(\eta) = \eta^{D/2} \chi_{\pm}(\eta), \quad (81)$$

equation (80) is reduced to the following form,

$$\left(\eta^2 \partial_0^2 + \eta \partial_0 + (p\eta)^2 - \left(\frac{im}{k} \pm \frac{1}{2} \right)^2 \right) \chi_{\pm} = 0. \quad (82)$$

Now we write the solutions of (82) as

$$\chi_{\pm}(\eta) = C_{\pm} H_{\frac{im}{k} \pm \frac{1}{2}}^{(2)}(p\eta) \quad (83)$$

where $H_{\nu}^{(2)}(x)$ are Hankel function of second kind of order ν . We only considered Hankel function of second kind as the solution for equation (82) because for positive energy solution in Bunch-Davies vacuum we demand $\psi^{(+)} \propto e^{-ip\eta}$ [34]. The coefficients C_+ and C_- are not independent of each other. We can find the relationship $C_- = -ip_b \sigma^b C_+ / p$ by inserting the solution matrices (83) and (81) into the equation (79). Moreover, we require additional quantum numbers apart from \mathbf{p} to specify all the solutions. In order to do that we need to fix the spinor C_+ . Here we take orthonormal basis for spinors by choosing $C_+ = C_{\beta}^{(+)} w^{(\sigma)}$, where $C_{\beta}^{(+)}$ is a normalization constant and $w^{(\sigma)}$,

$\sigma = 1, \dots, N/2$, are one-column matrices of $N/2$ rows, with elements $w_l^{(\sigma)} = \delta_{l\sigma}$. Combining with the negative energy solutions this set $\beta = (\mathbf{p}, \sigma)$ will form a complete set of quantum numbers. As a result, the positive-energy mode functions for Bunch-Davies vacuum takes the following form,

$$\psi_\beta^{(+)} = C_\beta^{(+)} \eta^{D/2} e^{i\mathbf{p}\mathbf{x}} \begin{bmatrix} w^{(\sigma)} k_{\frac{im}{k} + \frac{1}{2}}^{(2)}(p\eta) \\ -\frac{ip_b \sigma^b}{p} w^{(\sigma)} k_{\frac{im}{k} - \frac{1}{2}}^{(2)}(p\eta) \end{bmatrix}. \quad (84)$$

The coefficient $C_\beta^{(+)}$ in (84) is set on from the normalization condition (using inner product defined over constant time hypersurface) [35]

$$\langle \psi_\beta^{(+)}, \psi_{\beta'}^{(+)} \rangle = \int d^{D-1}x \sqrt{\frac{|g|}{g^{00}}} \psi_\beta^{(+)\dagger} \psi_{\beta'}^{(+)} = \delta(\mathbf{p} - \mathbf{p}') \delta_{\sigma\sigma'}. \quad (85)$$

After evaluating the inner product we find the normalization constant

$$C_\beta^{(+)} = \frac{\sqrt{p} k^{\frac{D-1}{2}} e^{-i\phi/2}}{\sqrt{8(2\pi)^{D-2}}} e^{\frac{m\pi}{2k}}. \quad (86)$$

where ϕ represents an arbitrary phase. The negative-energy mode functions $\psi_\beta^{(-)}$ can be imposing the condition that $\psi_\beta^{(-)} \propto e^{-i\mathbf{p}\mathbf{x} + ip\eta}$. By following the same procedure illustrated above we obtain the negative energy solution:

$$\psi_\beta^{(-)} = \frac{\sqrt{p} k^{\frac{D-1}{2}} e^{i\phi/2}}{\sqrt{8(2\pi)^{D-2}}} e^{-\frac{m\pi}{2k}} \eta^{D/2} e^{-i\mathbf{p}\mathbf{x}} \begin{bmatrix} w^{(\sigma)} H_{\frac{im}{k} + \frac{1}{2}}^{(1)}(p\eta) \\ \frac{ip_b \sigma^b}{p} w^{(\sigma)} H_{\frac{im}{k} - \frac{1}{2}}^{(1)}(p\eta) \end{bmatrix}. \quad (87)$$

In the above equation $H_\nu^{(1)}(x)$ are Hankel function of first kind of order ν . Therefore we have successfully evaluated the complete set of solutions for the Dirac equation (76). Now we can write arbitrary spinor solution $\Psi(x)$ in the operator form.

$$\Psi(x) = \sum_{\sigma=1}^{N/2} \int d\mathbf{p} \left(b_\sigma(\mathbf{p}) \psi_\sigma^{(+)}(\mathbf{p}, x) + d_\sigma^\dagger(\mathbf{p}) \psi_\sigma^{(-)}(\mathbf{p}, x) \right) \quad (88)$$

$$\bar{\Psi}(x) = \sum_{\sigma=1}^{N/2} \int d\mathbf{p} \left(b_\sigma^\dagger(\mathbf{p}, \lambda) \overline{\psi_\sigma^{(+)}(\mathbf{p}, x)} + d_\sigma(\mathbf{p}) \overline{\psi_\sigma^{(-)}(\mathbf{p}, x)} \right), \quad (89)$$

where

$$b_\sigma(\mathbf{p}) |0\rangle = d_\sigma(\mathbf{p}) |0\rangle = 0, \quad (90)$$

$$\bar{\psi} = \psi^\dagger \gamma^0, \quad (91)$$

$$\{b_\sigma(\mathbf{p}), b_{\sigma'}^\dagger(\mathbf{p}')\} = \delta(\mathbf{p} - \mathbf{p}') \delta_{\sigma\sigma'}, \quad (92)$$

$$\{d_\sigma(\mathbf{p}), d_{\sigma'}^\dagger(\mathbf{p}')\} = \delta(\mathbf{p} - \mathbf{p}') \delta_{\sigma\sigma'}. \quad (93)$$

Now we can have an explicit form of the Wightman functions of the fermionic field,

$$\begin{aligned}
S^+(x, x') &= \langle 0 | \Psi(x) \bar{\Psi}(x') | 0 \rangle = \sum_{\sigma} \int d\mathbf{p} \psi_{\sigma}^{(+)}(\mathbf{p}, x) \overline{\psi_{\sigma}^{(+)}(\mathbf{p}, x')} \\
&= \sqrt{\frac{\eta'}{\eta}} \left(i \left(\not{D} + \frac{\Gamma^0}{2\eta} \right) + m \right) \left(\mathcal{P}^+ G_{dS_D}(x, x', \frac{im}{k} - \frac{1}{2}) + \mathcal{P}^- G_{dS_D}(x, x', \frac{im}{k} + \frac{1}{2}) \right)
\end{aligned} \tag{94}$$

$$\begin{aligned}
S^-(x, x') &= \langle 0 | \bar{\Psi}(x') \Psi(x) | 0 \rangle = \sum_{\sigma} \int d\mathbf{p} \psi_{\sigma}^{(-)}(\mathbf{p}, x) \overline{\psi_{\sigma}^{(-)}(\mathbf{p}, x')} \\
&= -\sqrt{\frac{\eta'}{\eta}} \left(i \left(\not{D} + \frac{\Gamma^0}{2\eta} \right) + m \right) \left(\mathcal{P}^+ G_{dS_D}(x', x, \frac{im}{k} - \frac{1}{2}) + \mathcal{P}^- G_{dS_D}(x', x, \frac{im}{k} + \frac{1}{2}) \right)
\end{aligned} \tag{95}$$

where $P^{\pm} = (\mathbb{I}_{N \times N} \pm \gamma^0)/2$ and

$$G_{dS_D}(x, x', \frac{im}{k} \pm \frac{1}{2}) = \int d\mathbf{p} \frac{(\eta\eta')^{\frac{D-1}{2}} H^{D-2}}{8(2\pi)^{D-2}} e^{i\mathbf{p}(\mathbf{x}-\mathbf{x}')} H_{\frac{im}{k} \pm \frac{1}{2}}^{(2)}(p\eta) H_{\frac{m}{k} \pm \frac{1}{2}}^{(1)}(p\eta'). \tag{96}$$

Now the Wightman function for massless fermions in dS background,

$$S^{\pm}(x, x') = \pm i \sqrt{\frac{\eta'}{\eta}} \left(\not{D} + \frac{\Gamma^0}{2\eta} \right) G_{dS_D}(x, x') \tag{97}$$

and G_{dS_D} is as usual from equations (45-47) ,

$$G_{dS_D}(x, x') = G_{dS_D}(x', x, \frac{1}{2}) = G_{dS_D}(x, x', -\frac{1}{2}) = \frac{H^{D-2} \Gamma(D/2 - 1)}{2(2\pi)^{D/2}} v^{1-D/2}. \tag{98}$$

From equation (97) we can further deduce that

$$S^{\pm}(x, x') = \pm i \frac{H\eta_{ab}(x^a - x'^a)\gamma^b}{\sqrt{\eta\eta'}v} \left(\frac{D-2}{2} \right) G_{dS_D}(x, x') \tag{99}$$

The detector is moving in with constant linear acceleration a following (48) as before. In that case we know the detector response function of fermions (per unit time) for interaction Lagrangian is given by[27],

$$\mathcal{J}_{dS_D} = \int_{-\infty}^{\infty} d\Delta\tau e^{-iE\Delta\tau} S_D^{(2)}(\Delta\tau) \tag{100}$$

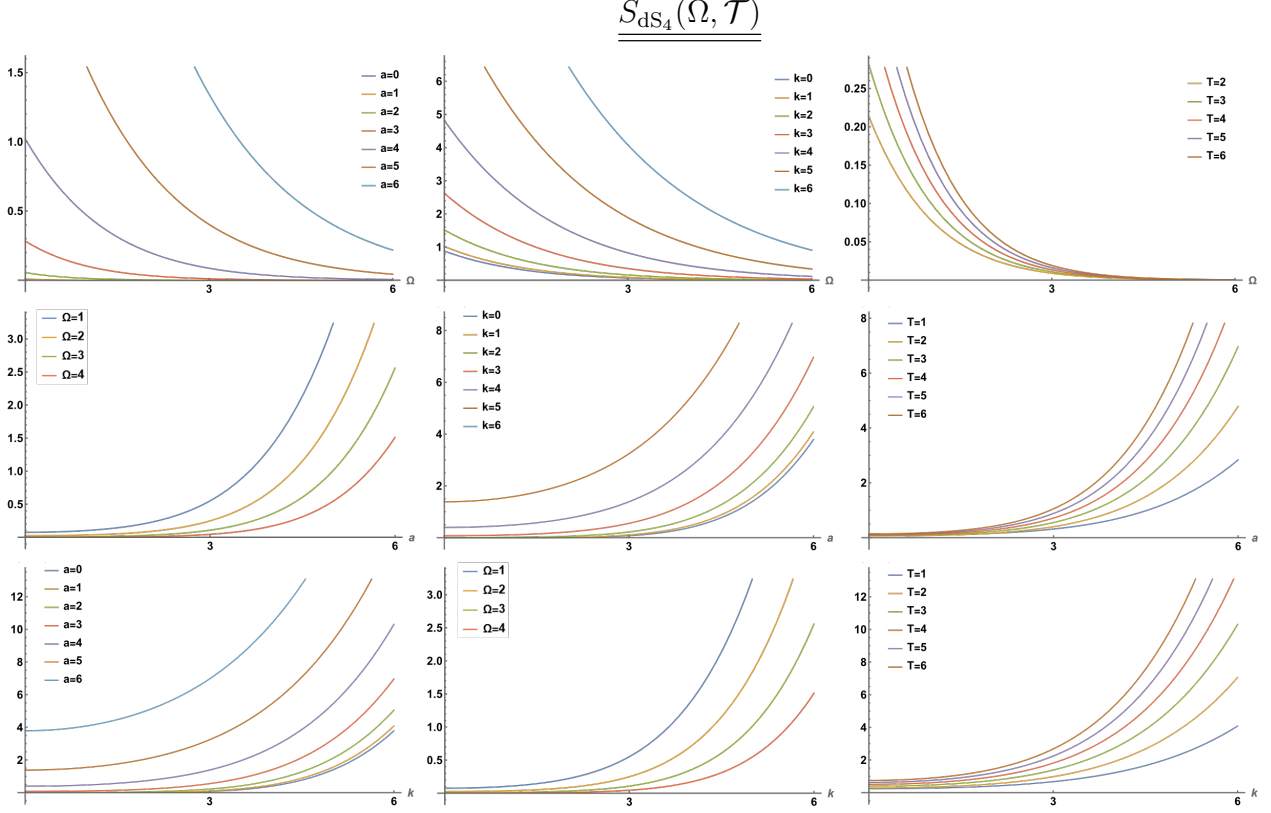


Figure 9: Plot of the Finite-Time response of the UDW Particle Detector in dS Space-time coupled to a fermionic Field. Each row (from top to bottom) shows the plot of the response function against Ω (varying $a[\mathcal{T} = 3, k = 3]$, $k[\mathcal{T} = 3, a = 3]$, $\mathcal{T}[a = 3, k = 3]$), against a (varying $\Omega[k = 3, \mathcal{T} = 3]$, $k[\Omega = 1, \mathcal{T} = 3]$, $\mathcal{T}[k = 3, \Omega = 1]$), and against k (varying $a[\Omega = 1, \mathcal{T} = 3]$, $\Omega[a = 3, \mathcal{T} = 3]$, $\mathcal{T}[a = 3, \Omega = 1]$) respectively.

where,

$$\begin{aligned}
S_D^{(2)}(x(\tau), x(\tau')) &= \langle 0 | : (\bar{\Psi}_a(x(\tau))) \Psi_a(x(\tau)) :: (\bar{\Psi}_b(x(\tau'))) \Psi_b(x(\tau')) : | 0 \rangle \\
&= \text{Tr}[S^+(x, x') S^-(x', x)] \\
&= k^2 \frac{\eta_{ab}(x^a - x'^a) \eta_{cd}(x^c - x'^c)}{\eta \eta' \nu^2} \text{Tr}[\gamma^b \gamma^d] \left(\frac{D-2}{2} \right)^2 G_{\text{dS}_D}(x, x') G_{\text{dS}_D}(x', x) \\
&= N k^2 (D/2 - 1)^2 \frac{\eta_{ab} \eta_{cd} \eta^{bd} (x^a - x'^a) (x'^c - x^c)}{\eta \eta' \nu^2} \frac{H^{2D-4} \Gamma(D/2 - 1)^2}{4(2\pi)^D} \nu^{2-D} \\
&= N \frac{[(D/2 - 1) \Gamma(D/2 - 1)]^2}{\Gamma(D - 1)} \left(\frac{k^{2D-2} \Gamma(D - 1)}{2(2\pi)^D} \right) \nu^{-D} \left(\frac{\eta_{ac} (x^a - x'^a) (x'^c - x^c)}{2\eta \eta'} \right) \\
&= N \frac{\Gamma(D/2)^2}{\Gamma(D - 1)} \left(\frac{k^{2D-2} \Gamma(D - 1)}{2(2\pi)^D} \right) \nu^{1-D} \\
&= N \frac{(\Gamma(D/2))^2}{\Gamma(D - 1)} G_{\text{dS}_{2D}}(x(\tau), x(\tau')).
\end{aligned} \tag{102}$$

is 4-points correlator of fermionic field. Here we are taking the trace over spinor index a, b , and, we have used the identity,

$$\text{Tr}[\gamma^b \gamma^d] = N \eta^{bd} \tag{103}$$

So the eq.102 dictates that in any of the path $S_D^{(2)}(\Delta\tau)$ takes the following form,

$$S_D^{(2)}(\Delta\tau) = N \frac{(\Gamma(D/2))^2}{\Gamma(D-1)} G_{\text{dS}_{2D}}(\Delta\tau) \quad (104)$$

From eq. (100) we can then conclude that detector response function for fermions can be related to response function for the scalars,

$$\mathcal{J}_{dS_D} = N \frac{(\Gamma(D/2))^2}{\Gamma(D-1)} \mathcal{F}_{\text{dS}_{2D}}^{(1)}. \quad (105)$$

Thus we have proved the following statement.

The response function of an UDW detector(with uniform linear acceleration) quadratically coupled to a massless Dirac field in (A)dS vacuum in $D \geq 2$ spacetime dimensions exactly equals to the response function of a UDW detector which is linearly coupled to a massless scalar field in $2D$ dimensional (A)dS vacuum times dimensional dependent numeric factor. Here, the fermionic field is minimally coupled to background while the scalar field is conformally coupled to the background.

Upon establishing the above statement for fermionic response in maximally symmetric spacetime we plot the response function in figure 8 and 9 with respect to different variables such as energy gap Ω , acceleration a and curvature k . We can also see the similar pattern in (A)dS fermionic response function that the response increases with increasing acceleration a but decreases as with increasing energy gap Ω . The response decreases with the increment curvature k in AdS and the opposite pattern is noticed in dS background. Also because of the fact 4 dimensional fermionic response function is related to higher (eight) dimensional scalar response function we find out, accelerated UDW detectors respond better when coupled to fermionic fields compared to bosonic fields.

3 Huygen's principle, detector and Unruh radiation

Huygen's principle is a well studied phenomenon specially in quantum field theory. It is a natural question to ponder whether the accelerated detectors observing the thermal radiation maintains the Huygen's principle[25]. The observed radiation from massless scalars by UDW detectors do not maintain the Huygen's principle in flat spacetime in three (odd) dimensions[25]. However this statement is well understood for accelerated UDW detectors in flat spacetime with linear coupling. But in this section we discuss the status of Huygen's principle for scalar theories where accelerated UDW detectors moving in the maximally symmetric curved spacetime with non linear interaction coupling(21)[24]. The Huygen's principle has several different equivalent definitions but we can work on with the following one [36, 37, 38]-

- i) The theory **maintains** the Huygen's principle if the causal propagator G_c has support only on the lightcone.
- ii) The theory **violates** the Huygen's principle if they are non vanishing elsewhere.

To understand better the state of Huygen's principle for the detected Unruh radiation we need to first fix the coupling between the detector and the matter field (23). For the usual linearly coupled ($n = 1$) detector, the response function simple depends upon the Wightman function. Concentrating on linear coupling, the causal propagator for conformally coupled scalar theory can



Figure 10: (A) Support of the propagators of a massless scalar in even dimensions for odd or even coupling associated with (21). This also depicts support of the propagators of a massless scalar in odd dimensions with even coupling. (B) Support of the propagators of a massless scalar in odd dimensions for odd coupling associated with (21)

defined as,

$$G^c(x, x') = W_D^{(2)}(x, x') - W_D^{(2)}(x', x) = \langle 0 | [\Phi(x), \Phi(x')] | 0 \rangle \quad (106)$$

In flat spacetime, the origin of obeying (or violating) the Huygen's principle can be explained for linearly coupled detector. In case of the linear coupling the detector response function is nothing but the Fourier transform of the Wightman function $W_D^{(2)}(x, x')$, which is proportional to $L^{1-\frac{d}{2}}$ for a bosonic field. Here L is the square distance between the two points x and x' . Now when the two point function is analytically continued to complex τ there is a branch cut for timelike distance when we are in odd dimensions. This branch cut becomes a simple pole in even dimensions. Therefore when we compute the response function in odd dimensions using (22) the linear detector finds a branch cut in the integral expression and therefore reports a Fermi-Dirac distribution. The support of the propagator of scalar fields for linear detector[25] can be exactly (23) analysed with figure 10A. For even dimensions, the support of G_c is only on the lightcone while in odd dimension the support of G_c is on the entire timelike region. In the case of conformally coupled scalar fields over (A)dS spacetime, we can follow the same argument as before. For example, the two point correlator of conformally coupled scalars in dS can be simply related to flat space correlator $W_M^{(2)}(x, x')$ using the followings relation[35, 39],

$$W_{dS}^{(2)}(x, x') = (k^2 \eta^2)^{\frac{d-2}{4}} W_M^{(2)}(x, x') (k^2 \eta'^2)^{\frac{d-2}{4}} \quad (107)$$

Therefore the pole structure for conformally coupled theories are similar to those of flat spacetime. In even dimensional flat spacetime the causal correlator is given by[38],

$$G_c = [\Phi(t, \vec{x}), \Phi(t + \Delta t, \vec{x} + \Delta \vec{x})] = \frac{i}{4\pi \Delta \vec{x}} [\delta(\Delta \vec{t} + \Delta \vec{x}) - \delta(\Delta \vec{t} - \Delta \vec{x})] \quad (108)$$

In similar fashion with odd dimensional spacetime $D = d + 1^4$, it is given by

$$G_c = [\Phi(t, \vec{x}), \Phi(t + \Delta t, \vec{x} + \Delta \vec{x})] = \frac{\Gamma(\frac{d-1}{2})}{4\pi^{\frac{d+1}{2}}} \frac{1}{L^{\frac{d-1}{2}}} \quad (109)$$

⁴even dimensional space d .

We can see from eq. (108) that in even dimensional Minkowski spacetime the support of G_c is exactly on the lightcone while in odd dimensional spacetime the support of G_c is also inside the lightcone. Exactly similar result will hold for conformally coupled scalar theory living on (A)dS background through (107). We now go ahead and generalize the results with coupling $n \geq 1$. The causal propagator can be written for any coupling n in this fashion,

$$G^c(x, x') = W^{(2n)}(x, x') - W^{(2n)}(x', x) \quad (110)$$

The $2n$ point correlators are related to two point correlators using (52). And thus the pole structure of $2n$ point correlator can be easily understood using this relation. In odd dimension the branch cut in Wightman function results a branch cut in $2n$ point correlator for any odd coupling n . However when we choose the even coupling the branch cut turns into simple pole for the $2n$ point correlator. Huygen's principle for scalar fields are therefore obeyed as well as no statistics inversion is noticed by the Unruh radiation in odd dimension only when we choose the even coupling. On the contrary the Huygen's principle is violated in odd dimensions with odd coupling and statistics inversion also happens.

In case of even coupling, the pole structure of the $2n$ -point correlator function are also quite interesting. Through (52) focusing in even dimensions, the Wightman function has no branch cut in even dimensions. Therefore for any even coupling the $2n$ -point correlators will not have any surprise branch cut in even dimensions. So, the Huygen's principle is going to be satisfied trivially. However, in odd dimensions there is a branch cut in Wightman function. But in the $2n$ -point correlator, when we use (52) it immediately suggests the branch cut turns to a simple pole for any even n . As a result for even n , the Unruh radiation of scalars in flat space as well as in conformally coupled maximally symmetric scalar solutions the Huygen's principle is always maintained in any dimensions. It is not possible to violate Huygen's principle if we choose coupling with even n . The support of the scalar solutions are surprisingly always on the lightcone for even coupling. Figure 10(A) accurately depicts the status Huygen's Principle in scalar Unruh radiation with odd coupling and odd dimesnions, where the support is just on the light cone. Interesting to see this is the exact situation when the statistics inversion happens through (54). In odd dimensions scalar theory propagator under consideration is anti-periodic in $\beta = \frac{2\pi}{\omega}$ when we choose odd coupling. In any other scenario the $2n$ point propagator is periodic in β where the Hugen's principle is perfectly maintained in Unruh radiation.

Let us now focus our discussion on the Huygen's principle for fermionic theory with interaction Hamiltonian (61). This is the most commonly used interaction Hamiltonian between fermionic theory and detector[22]. Now the definition of Huygen principle (written before eq. (106)) remains the same for fermionic theory as well but the definition of G_c is given by Anti-Commutator instead of commutator algebra as in (106)⁵,

$$G^c(x, x') = \langle 0 | \{ \chi(x), \chi(x') \} | 0 \rangle \quad (111)$$

where,

$$\chi(x) =: \bar{\Psi}_a(x) \Psi_a(x) : \quad (112)$$

The study of support for fermionic correlator on lightcone is a bit troublesome specially in the curved spacetime because of the gamma matrices. For the interaction Hamiltonian given by (61), the

⁵where the trace over spin index is assumed



Figure 11: Support of the four point propagators of a massless fermions in any dimensions for interaction Hamiltonian (60). This is the clear indication that Huygen's principle is always maintained for fermions.

detector response function is dependent upon the four point fermionic correlator as seen explicitly from (62). In ref.[25], the author focused on the two point function of fermionic fields to understand the status of Huygen's principle of the Unruh radiation detected by the Unruh-DeWitt detectors instead of the four point function. As a result, it was concluded in ref.[25] that the Unruh radiation detected for fermions maintain Huygen's principle in odd dimensions while violate it in even dimensions. Because the pole and branch cut structure of four point fermionic correlator is quite different to the two point correlator. In case of flat space[22], AdS[23] as well as in dS ((105)), one can easily see that four point fermionic correlators in D dimensions is explicitly given by the two point scalar correlators in $2D$ dimensions. Therefore to understand the status of Huygen's principle for Unruh radiation of the fermionic theory (60) in odd or even D dimension, we can instead think of the massless scalars in $2D$ dimensions. The scalar Wightman function when conformally coupled to the background (A)dS gravity solutions has no branch cut in even dimensions. As a consequence, the 4-point fermionic propagator, to which the detector is sensitive always have support only on the light cone. It is quite surprising to see that scalar theory fails to maintain the Huygen principle in odd dimensions with usual linear coupling while the fermionic theory always maintains the Huygen principle with the usual interaction Hamiltonian(60). This result is true for matter fields in flat spacetime as well as conformally coupled to maximally symmetric spacetimes. The reason behind the conclusion being different to Huygen's principle of fermionic Unruh radiation in ref.[25] is because they performed their analysis with two point function. But for the interaction Hamiltonian (60)⁶, one should actually analyse the four point fermionic correlator. Because the detector response is dependent on four point fermionic correlator rather than the fermionic Wightman function (see (62)), the correlator under consideration maintains a periodic condition with periodicity $\beta = \frac{2\pi}{\omega}$ and the Huygen's principle is always maintained the irrespective of dimensionality of spacetime.

4 Discussion and future works

In this article we have completed the computation of finite time response of accelerated UDW detectors in maximally symmetric spacetime. The behaviour of the response function with different parameters are systematically analysed in figure (2) - (9). We also concluded the analysis

⁶see 2.15b no eq. of [25], where they use the same interaction Hamiltonian.

for fermionic response function in maximally symmetric background (see the boxed statement after (105)). The result is quite powerful which also allows us to determine the status of Huygen's principle of the fermionic Unruh radiation detected by UDW detector moving in maximally symmetric spacetime. It is quite intriguing to note that the Huygen's principle is always maintained in fermionic Unruh radiation which is minimally coupled to background as opposed to minimally coupled scalar[15]. We are currently working on to see if such results of fermionic response also holds when the UDW detectors are moving in other interesting curved spacetime solutions such as blackholes. As an application of finite time response we would also like to construct Unruh Otto engines[20] with the help of UDW detectors moving in maximally symmetric backgrounds. The variation of response function in dS and AdS space with respect to curvature makes the situation quite interesting and we are focusing on explicit conditions to extract required conditions for completing Otto cycle to have positive work output. The recent claim that with entangled qubits one can build up more efficient[40, 41] Otto engine is quite exciting and we are exploring the possibility to generalise it with maximally symmetric spacetimes. In our current manuscript, we have worked with scalar theory which is conformally coupled to background gravity but we are in a process of computing the finite time response function of UDW detectors for minimally coupled scalar theory[42].

5 Appendix: Constant Acceleration Path in dS spacetime

Here, we show that the path considered in eq. 48 is a constant acceleration path. The components of the acceleration can be written as,

$$a^\mu = \frac{d^2 x^\mu}{d\tau^2} + 2\Gamma_{\alpha\beta}^\mu \left(\frac{dx^\alpha}{d\tau} \right) \left(\frac{dx^\beta}{d\tau} \right) \quad (113)$$

where, $\Gamma_{\alpha\beta}^\mu$ are Christoffel symbols of the first kind. Writing the components out explicitly for the path in eq. 48, we have,

$$\begin{aligned} a^{(0)} &= \frac{d^2 \eta}{d\tau^2} + 2\Gamma_{\alpha\beta}^0 \left(\frac{dx^\alpha}{d\tau} \right) \left(\frac{dx^\beta}{d\tau} \right) \\ &= \frac{d^2 \eta}{d\tau^2} - \frac{1}{\tau} \left(\frac{d\eta}{d\tau} \right)^2 - \frac{1}{\tau} \left(\frac{dx^1}{d\tau} \right)^2 \\ &= \tau_0 \omega^2 e^{\omega\tau} - \frac{1}{\tau_0 e^{\omega\tau}} (\tau_0 \omega e^{\omega\tau})^2 - \frac{1}{\tau_0 e^{\omega\tau}} \left(\frac{a\tau_0}{\omega} \omega e^{\omega\tau} \right)^2 \\ &= -a^2 \tau_0 e^{\omega\tau} \end{aligned} \quad (114)$$

$$\begin{aligned} a^{(1)} &= \frac{d^2 x^1}{d\tau^2} + 2\Gamma_{\alpha\beta}^1 \left(\frac{dx^\alpha}{d\tau} \right) \left(\frac{dx^\beta}{d\tau} \right) \\ &= \frac{d^2 x^1}{d\tau^2} - \frac{2}{\tau} \frac{dx^1}{d\tau} \frac{d\eta}{d\tau} \\ &= \frac{a\tau_0}{\omega} \omega^2 e^{\omega\tau} - \frac{2}{\tau_0 e^{\omega\tau}} \left(\frac{a\tau_0}{\omega} \omega e^{\omega\tau} \right) (\tau_0 \omega e^{\omega\tau}) \\ &= -a\tau_0 \omega e^{\omega\tau} \end{aligned} \quad (115)$$

$$a^{(2)} = a^{(3)} = \dots = a^{(D-1)} = 0 \quad (116)$$

So, the magnitude of the acceleration \mathbf{a} becomes,

$$\begin{aligned}
|\mathbf{a}|^2 &= -a_\mu a^\mu \\
&= -g_{00}(a^0)^2 - g_{11}(a^1)^2 \\
&= -\frac{1}{H^2\tau^2}a^4\tau_0^2e^{2\omega\tau} + \frac{1}{H^2\tau^2}a^2\tau_0^2\omega^2e^{2\omega\tau} \\
&= -\frac{1}{H^2\tau_0^2e^{2\omega\tau}}a^2\tau_0^2e^{2\omega\tau}(a^2 - \omega^2) \\
&= a^2
\end{aligned} \tag{117}$$

Hence, $|\mathbf{a}| = a$ and the acceleration along this path is uniform.

6 Acknowledgments

MMF's research is supported by NSERC and in part by the Delta Institute of Theoretical Physics. The authors would like to thank Sowmitra Das and Onirban Islam for the discussions.

References

- [1] Stanley Deser and Orit Levin. Mapping hawking into unruh thermal properties. *Physical Review D*, 59(6):064004, 1999.
- [2] Stanley Deser and Orit Levin. Accelerated detectors and temperature in (anti) de sitter spaces. *Classical and Quantum Gravity*, 14(L163), 1997.
- [3] Stanley Deser and Orit Levin. Equivalence of hawking and unruh temperatures and entropies through flat space embeddings. *Classical and Quantum Gravity*, 15(12):L85, 1998.
- [4] Thanu Padmanabhan. Cosmological constant—the weight of the vacuum. *Physics Reports*, 380(5-6):235–320, 2003.
- [5] Thanu Padmanabhan. Gravity and the thermodynamics of horizons. *Physics Reports*, 406(2):49–125, 2005.
- [6] David Jennings. On the response of a particle detector in Anti-de Sitter spacetime. *Class. Quant. Grav.*, 27:205005, 2010. doi: 10.1088/0264-9381/27/20/205005.
- [7] Grant Salton, Robert B Mann, and Nicolas C Menicucci. Acceleration-assisted entanglement harvesting and rangefinding. *New Journal of Physics*, 17(3):035001, 2015.
- [8] Keith K Ng, Robert B Mann, and Eduardo Martín-Martínez. New techniques for entanglement harvesting in flat and curved spacetimes. *Physical Review D*, 97(12):125011, 2018.
- [9] Erickson Tjoa and Eduardo Martín-Martínez. When entanglement harvesting is not really harvesting. *Physical Review D*, 104(12):125005, 2021.
- [10] Héctor Maeso-García, T Rick Perche, and Eduardo Martín-Martínez. Entanglement harvesting: Detector gap and field mass optimization. *Physical Review D*, 106(4):045014, 2022.
- [11] Elena Cáceres, Mariano Chernicoff, Alberto Güijosa, and Juan F Pedraza. Quantum fluctuations and the unruh effect in strongly-coupled conformal field theories. *Journal of High Energy Physics*, 2010(6):1–30, 2010.
- [12] Andreas Blommaert, Thomas G Mertens, and Henri Verschelde. Unruh detectors and quantum chaos in jt gravity. *Journal of High Energy Physics*, 2021(3):1–37, 2021.

- [13] Aindriú Conroy. Unruh-dewitt detectors in cosmological spacetimes. *arXiv preprint arXiv:2204.00359*, 2022.
- [14] Eduardo Martin-Martinez and Nicolas C Menicucci. Cosmological quantum entanglement. *Classical and Quantum Gravity*, 29(22):224003, 2012.
- [15] Ana Blasco, Luis J. Garay, Mercedes Martin-Benito, and Eduardo Martin-Martinez. Violation of the Strong Huygen’s Principle and Timelike Signals from the Early Universe. *Phys. Rev. Lett.*, 114(14):141103, 2015. doi: 10.1103/PhysRevLett.114.141103.
- [16] Jiatong Yan and Baocheng Zhang. Effect of spacetime dimensions on quantum entanglement between two uniformly accelerated atoms. *Journal of High Energy Physics*, 2022(10):1–29, 2022.
- [17] Anshuman Bhardwaj and Daniel E. Sheehy. Unruh Effect and Takagi’s Statistics Inversion in Strained Graphene. 9 2022.
- [18] Satoshi Ohya. Emergent anyon distribution in the unruh effect. *Physical Review D*, 96(4):045017, 2017.
- [19] Enrique Arias, Thiago R. de Oliveira, and M. S. Sarandy. The Unruh Quantum Otto Engine. *JHEP*, 02:168, 2018. doi: 10.1007/JHEP02(2018)168.
- [20] Finnian Gray and Robert B Mann. Scalar and fermionic unruh otto engines. *Journal of High Energy Physics*, 2018(11):1–34, 2018.
- [21] Shin Takagi. Vacuum noise and stress induced by uniform acceleration hawking-unruh effect in rindler manifold of arbitrary dimension. *Progress of Theoretical Physics Supplement*, 88:1–142, 1986.
- [22] Jorma Louko and Vladimir Toussaint. Unruh-dewitt detector’s response to fermions in flat spacetimes. *Physical Review D*, 94(6):064027, 2016.
- [23] Shahnewaz Ahmed and Mir Mehedi Faruk. Accelerated paths and unruh effect. part i. scalars and fermions in anti de sitter spacetime. *Journal of High Energy Physics*, 2021(9):1–46, 2021.
- [24] L. Sriramkumar. Odd statistics in odd dimensions for odd couplings. *Mod. Phys. Lett. A*, 17:1059–1066, 2002. doi: 10.1142/S0217732302007545.
- [25] Hiroshi Ooguri. Spectrum of Hawking Radiation and Huygens’ Principle. *Phys. Rev. D*, 33:3573, 1986. doi: 10.1103/PhysRevD.33.3573.
- [26] L. Sriramkumar and T. Padmanabhan. Response of finite time particle detectors in noninertial frames and curved space-time. *Class. Quant. Grav.*, 13:2061–2079, 1996. doi: 10.1088/0264-9381/13/8/005.
- [27] Steven Weinberg. *Gravitation and cosmology: principles and applications of the general theory of relativity*. 1972.
- [28] Ivan M. Burbano, T. Rick Perche, and Bruno de S. L. Torres. A path integral formulation for particle detectors: the Unruh-DeWitt model as a line defect. *JHEP*, 03:076, 2021. doi: 10.1007/JHEP03(2021)076.
- [29] Ashok Das. *Lectures on quantum field theory*. World Scientific, 2020.
- [30] Sean M. Carroll. *Spacetime and Geometry*. Cambridge University Press, 7 2019. ISBN 978-0-8053-8732-2, 978-1-108-48839-6, 978-1-108-77555-7.

- [31] Shin Takagi. Vacuum noise and stress induced by uniform accelerationhawking-unruh effect in rindler manifold of arbitrary dimension. *Progress of Theoretical Physics Supplement*, 88: 1–142, 1986.
- [32] Raphael Bousso, Alexander Maloney, and Andrew Strominger. Conformal vacua and entropy in de sitter space. *Physical Review D*, 65(10):104039, 2002.
- [33] Shahnewaz Ahmed and Mir Mehedi Faruk. Accelerated paths and unruh effect. part i. scalars and fermions in anti de sitter spacetime. *Journal of High Energy Physics*, 2021(9):1–46, 2021.
- [34] Hael Collins. Fermionic α -vacua. *Physical Review D*, 71(2):024002, 2005.
- [35] AA Saharian. Quantum field theory in curved spacetime, 2020.
- [36] Karen Yagdjian. Huygens’ principle for the generalized Dirac operator in curved spacetime. *J. Phys. A*, 54(9):095204, 2021. doi: 10.1088/1751-8121/abdde9.
- [37] Gunther Paul. *Huygens’ principle and hyperbolic equations*. Academic Press, 2014.
- [38] Robert H. Jonsson. Decoupling of Information Propagation from Energy Propagation. *PhD Thesis, University of Waterloo*, 20156.
- [39] Marino Marcos. Qft in curved space, 2020.
- [40] Dipankar Barman and Bibhas Ranjan Majhi. Constructing an entangled Unruh Otto engine and its efficiency. *JHEP*, 05:046, 2022. doi: 10.1007/JHEP05(2022)046.
- [41] Gaurang Ramakant Kane and Bibhas Ranjan Majhi. Entangled quantum Unruh Otto engine is more efficient. *Phys. Rev. D*, 104(4):041701, 2021. doi: 10.1103/PhysRevD.104.L041701.
- [42] Bjorn Garbrecht and Tomislav Prokopec. Unruh response functions for scalar fields in de Sitter space. *Class. Quant. Grav.*, 21:4993–5004, 2004. doi: 10.1088/0264-9381/21/21/016.